

Sharp bounds of constants in Poincaré-type inequalities for simplicial domains

S. Matculevich and S. Repin

Department of Mathematical Information Technology, University of Jyväskylä
 FIN-40100 Jyväskylä, FINLAND
 e-mails: svetlana.v.matculevich@jyu.fi, sergey.repin@jyu.fi

St. Petersburg Dept. of V.A. Steklov Institute of Mathematics of RAS
 St. Petersburg, Russia

September 6, 2018

Abstract

The paper is concerned with sharp estimates of constants in classical Poincaré inequalities and Poincaré-type inequalities for functions having zero mean value in a simplicial domain or on a part of its boundary. These estimates are important for quantitative analysis of problems generated by differential equations, where numerical approximations are typically constructed with the help of simplicial meshes. We suggest easily computable relations that provide sharp bounds of the respective constants and compare these results with analytical estimates (if they are known). In the last section, we present an example that shows possible applications of the results and derive a computable majorant of the difference between the exact solution of a boundary value problem and an arbitrary finite dimensional approximation computed on a simplicial mesh, which uses above mentioned constants.

1 Introduction

Let T be a bounded domain in \mathbb{R}^d ($d \geq 2$) with Lipschitz boundary ∂T . It is well known that the Poincaré inequality ([32, 33])

$$\|w\|_T \leq C_T^P \|\nabla w\|_T \quad (1)$$

holds for any

$$w \in \tilde{H}^1(T) := \left\{ w \in H^1(T) \mid \{w\}_T = 0 \right\},$$

where $\|w\|_T$ denotes the norm in $L^2(T)$, $\{w\}_T := \frac{1}{|T|} \int_T w \, dx$ is the mean value of w over T , and $|T|$ is the Lebesgue measure of T . The constant C_T^P depends only on T and d .

Poincaré-type inequalities also hold for

$$w \in \tilde{H}^1(T, \Gamma) := \left\{ w \in H^1(T) \mid \{w\}_\Gamma = 0 \right\},$$

where Γ is a measurable part of ∂T such that $\text{meas}_{d-1} \Gamma > 0$ (in particular, Γ may coincide with the whole boundary). For any $w \in \tilde{H}^1(T, \Gamma)$, we have two inequalities similar to (1). The first one

$$\|w\|_T \leq C_\Gamma^P \|\nabla w\|_T \quad (2)$$

is another form of the Poincaré inequality (1), which is stated for a different set of functions and contains a different constant, i.e. $C_T^P \leq C_\Gamma^P$. The constant C_Γ^P is associated with the minimal positive eigenvalue of the problem

$$-\Delta u = \lambda u \text{ in } T; \quad \partial_n u = \lambda \{u\}_T \text{ on } \Gamma; \quad \partial_n u = 0 \text{ on } \partial T \setminus \Gamma; \quad \forall u \in \tilde{H}^1(T, \Gamma). \quad (3)$$

We note that inequalities of this type arose in finite element analysis many years ago (see, e.g., [2]), where (2) was considered for simplexes in \mathbb{R}^2 . The second inequality

$$\|w\|_\Gamma \leq C_\Gamma^{\text{Tr}} \|\nabla w\|_T \quad (4)$$

estimates the trace of $w \in \tilde{H}^1(T, \Gamma)$ on Γ . It is associated with the minimal nonzero eigenvalue of the problem

$$-\Delta u = 0 \text{ in } T; \quad \partial_n u = \lambda u \text{ on } \Gamma; \quad \partial_n u = 0 \text{ on } \partial T \setminus \Gamma; \quad \forall u \in \tilde{H}^1(T, \Gamma). \quad (5)$$

The problem (5) is a special case of the Steklov problem [39], where the spectral parameter appears in the boundary condition. Sometimes (5) is associated with the so-called *sloshing problem*, which describes oscillations of a fluid in a container. Eigenvalues and eigenfunctions of the sloshing problem have been studied in [13, 4, 17, 18, 19, 14] and some other papers cited therein.

Exact values of C_Γ^P , C_Γ^{Tr} , and C_T^P are important from both analytical and computational points of view. Poincaré-type inequalities are often used in analysis of nonconforming approximations (e.g., discontinuous Galerkin or mortar methods), domain decomposition methods (see, e.g., [16, 12] and [41]), a posteriori estimates [37], and other applications related to quantitative analysis of partial differential equations. Analysis of interpolation constants and their estimates for piecewise constant and linear interpolations over triangular finite elements can be found in [23] and literature cited therein. Finally, we note that [8] introduces a method of computing lower bounds for the eigenvalues of the Laplace operator based on nonconforming (Crouzeix-Raviart) approximations. This method yields guaranteed upper bounds of the constant in the Friedrichs' inequality.

It is known (see [30]) that for convex domains

$$C_T^P \leq \frac{\text{diam}(T)}{\pi}.$$

For triangles this estimate was improved in [22] to

$$C_T^P \leq \frac{\text{diam}(T)}{j_{1,1}},$$

where $j_{1,1} \approx 3.8317$ is the smallest positive root of the Bessel function J_1 . Moreover, for isosceles triangles from [3, 22] it follows that

$$C_T^P \leq \bar{C}_T^{P,\Delta} := \text{diam}(T) \cdot \begin{cases} \frac{1}{j_{1,1}} & \alpha \in (0, \frac{\pi}{3}], \\ \min \left\{ \frac{1}{j_{1,1}}, \frac{1}{j_{0,1}} (2(\pi - \alpha) \tan(\frac{\alpha}{2}))^{-1/2} \right\} & \alpha \in (\frac{\pi}{3}, \frac{\pi}{2}], \\ \frac{1}{j_{0,1}} (2(\pi - \alpha) \tan(\frac{\alpha}{2}))^{-1/2} & \alpha \in (\frac{\pi}{2}, \pi). \end{cases} \quad (6)$$

Here, $j_{0,1} \approx 2.4048$ is the smallest positive root of the Bessel function J_0 . A lower bound of C_T^P for convex domains in \mathbb{R}^2 was derived in [10] and it reads

$$C_T^P \geq \frac{\text{diam}(T)}{2j_{0,1}}. \quad (7)$$

Analogously, work [21] provides lower bound

$$C_T^P \geq \frac{P}{4\pi}, \quad (8)$$

which improves (7) for some cases. Here, P is perimeter of T .

In [29], exact values of C_Γ^P and C_Γ^{Tr} are found for parallelepipeds, rectangles, and right triangles. Subsequently, we exploit the following two results:

1. If T is based on vertexes $A = (0, 0)$, $B = (h, 0)$, $C = (0, h)$ and $\Gamma := \{x_1 \in [0, h], x_2 = 0\}$ (i.e., Γ coincides with one of the legs of the isosceles right triangle), then

$$C_\Gamma^P = \frac{h}{\zeta_0} \quad \text{and} \quad C_\Gamma^{\text{Tr}} = \left(\frac{h}{\zeta_0 \tanh(\hat{\zeta}_0)} \right)^{1/2}, \quad (9)$$

where ζ_0 and $\hat{\zeta}_0$ are unique roots of the equations

$$z \cot(z) + 1 = 0 \quad \text{and} \quad \tan(z) + \tanh(z) = 0, \quad (10)$$

respectively, in the interval $(0, \pi)$.

2. If T is based on vertexes $A = (0, 0)$, $B = (h, 0)$, $C = (\frac{h}{2}, \frac{h}{2})$, and Γ coincides with the hypotenuse of the isosceles right triangle, then

$$C_\Gamma^P = \frac{h}{2\zeta_0} \quad \text{and} \quad C_\Gamma^{\text{Tr}} = \left(\frac{h}{2} \right)^{1/2}.$$

It is worth emphasizing that values of C_Γ^{Tr} for right isosceles triangles follow from the exact solutions of the Steklov problem related to the square. This specific case was discussed in the work [14].

Exact value of constants in the classical Poincaré inequality are also known for certain triangles:

1. For the equilateral triangle $\widehat{T}_{\pi/3}$ based on vertexes $\hat{A} = (0,0)$, $\hat{B} = (1,0)$, $\hat{C} = (\frac{1}{2}, \frac{\sqrt{3}}{2})$, where $\hat{\Gamma} := \{x_1 \in [0, 1]; x_2 = 0\}$, the constant

$$C_{\widehat{T}, \pi/3}^P = \frac{3}{4\pi}$$

is derived in [31].

2. For the right isosceles triangles $\widehat{T}_{\pi/4}$ based on vertexes $\hat{A} = (0,0)$, $\hat{B} = (1,0)$, $\hat{C} = (\frac{1}{2}, \frac{1}{2})$ and $\widehat{T}_{\pi/2}$ based on $\hat{A} = (0,0)$, $\hat{B} = (1,0)$, $\hat{C} = (0,1)$, we have

$$C_{\widehat{T}, \pi/4}^P = \frac{1}{\sqrt{2}\pi} \quad \text{and} \quad C_{\widehat{T}, \pi/2}^P = \frac{1}{\pi},$$

respectively. Proofs can be found in [15] and [28].

Explicit formulas of the same constants for certain three-dimensional domains are presented in papers [5] and [15].

The above mentioned results form a basis for deriving sharp bounds of the constants C_{Γ}^P , C_{Γ}^{Tr} , and C_T^P for arbitrary non-degenerate triangles and tetrahedrons, which are typical objects in various discretization methods. In Section 2, we deduce guaranteed and easily computable bounds of C_{Γ}^P , C_{Γ}^{Tr} , and C_T^P for triangular domains. The efficiency of these bounds is tested in Section 3, where C_{Γ}^P and C_{Γ}^{Tr} are compared with lower bounds computed numerically by solving a generalized eigenvalue problem generated by Rayleigh quotients discretized over sufficiently representative sets of trial functions. In the same section, we make a similar comparison of numerical lower bounds related to the constant C_T^P with obtained upper bounds and existing estimates known from [21, 22] and [10]. Lower bounds of the constants presented in Section 3 have been computed by two independent codes: the first code is based on the MATLAB Symbolic Math Toolbox [40], and the second one uses The FEniCS Project [24]. Section 4 is devoted to tetrahedrons. We combine numerical and theoretical estimates in order to derive two-sided bounds of the constants. Finally, in Section 5 we present an example that shows one possible application of the estimates considered in previous sections. Here, the constants are used in order to deduce a guaranteed and fully computable upper bound of the distance between the exact solution of an elliptic boundary value problem and an arbitrary function (approximation) in the respective energy space.

2 Majorants of C_{Γ}^P and C_{Γ}^{Tr} for triangular domains

Let T be based on vertexes $A = (0,0)$, $B = (h,0)$, and $C = (h\rho \cos \alpha, h\rho \sin \alpha)$ and

$$\Gamma := \{x_1 \in [0, h]; x_2 = 0\}, \quad (11)$$

where $\rho > 0$, $h > 0$, and $\alpha \in (0, \pi)$ are geometrical parameters that fully define a triangle T (see Fig. 1). Easily computable bounds of C_{Γ}^P and C_{Γ}^{Tr} are presented in Lemma 1 below, which uses mappings of reference triangles to T and well-known integral transformations (see, e.g., [11]).

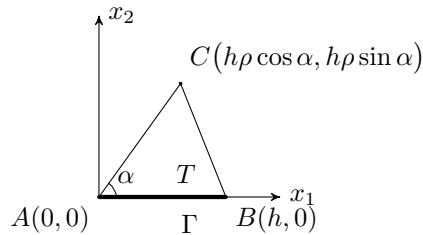


Figure 1: Simplex in \mathbb{R}^2 .

Lemma 1 For any $w \in \widetilde{H}^1(T, \Gamma)$, the upper bounds of constants in the inequalities

$$\|w\|_T \leq C_{\Gamma}^P h \|\nabla w\|_T \quad \text{and} \quad \|w\|_{\Gamma} \leq C_{\Gamma}^{\text{Tr}} h^{1/2} \|\nabla w\|_T \quad (12)$$

are defined as

$$C_{\Gamma}^P \leq \overline{C}_{\Gamma}^P = \min \left\{ \gamma_{\pi/2}^P C_{\widehat{\Gamma}, \pi/2}^P, \gamma_{\pi/4}^P C_{\widehat{\Gamma}, \pi/4}^P \right\} \quad \text{and} \quad C_{\Gamma}^{\text{Tr}} \leq \overline{C}_{\Gamma}^{\text{Tr}} = \min \left\{ \gamma_{\pi/2}^{\text{Tr}} C_{\widehat{\Gamma}, \pi/2}^{\text{Tr}}, \gamma_{\pi/4}^{\text{Tr}} C_{\widehat{\Gamma}, \pi/4}^{\text{Tr}} \right\},$$

respectively. Here,

$$\gamma_{\pi/2}^P = \mu_{\pi/2}^{1/2}, \quad \gamma_{\pi/4}^P = \mu_{\pi/4}^{1/2}, \quad \gamma_{\pi/2}^{\text{Tr}} = (\rho \sin \alpha)^{-1/2} \gamma_{\pi/2}^P, \quad \gamma_{\pi/4}^{\text{Tr}} = (2\rho \sin \alpha)^{-1/2} \gamma_{\pi/4}^P,$$

where

$$\mu_{\pi/2}(\rho, \alpha) = \frac{1}{2} \left(1 + \rho^2 + (1 + \rho^4 + 2\rho^2 \cos 2\alpha)^{1/2} \right), \quad (13)$$

$$\mu_{\pi/4}(\rho, \alpha) = 2\rho^2 - 2\rho \cos \alpha + 1 + ((2\rho^2 + 1)(2\rho^2 + 1 - 4\rho \cos \alpha + 4\rho^2 \cos 2\alpha))^{1/2}, \quad (14)$$

and $C_{\hat{\Gamma}, \pi/2}^P \approx 0.49291$, $C_{\hat{\Gamma}, \pi/2}^{\text{Tr}} \approx 0.65602$ and $C_{\hat{\Gamma}, \pi/4}^P \approx 0.24646$, $C_{\hat{\Gamma}, \pi/4}^{\text{Tr}} \approx 0.70711$, where $\hat{\Gamma}$ is defined as

$$\hat{\Gamma} := \{x_1 \in [0, 1]; x_2 = 0\}. \quad (15)$$

Proof: Consider the linear mapping $\mathcal{F}_{\pi/2} : \hat{T}_{\pi/2} \rightarrow T$ with

$$x = \mathcal{F}_{\pi/2}(\hat{x}) = B_{\pi/2} \hat{x}, \quad \text{where } B_{\pi/2} = \begin{pmatrix} h & \rho h \cos \alpha \\ 0 & \rho h \sin \alpha \end{pmatrix}, \quad \det B_{\pi/2} = \rho h^2 \sin \alpha.$$

For any $\hat{w} \in \tilde{H}^1(\hat{T}_{\pi/2}, \hat{\Gamma})$, we have the estimate

$$\|\hat{w}\|_{\hat{T}_{\pi/2}} \leq C_{\hat{\Gamma}, \pi/2}^P \|\nabla \hat{w}\|_{\hat{T}_{\pi/2}}, \quad (16)$$

where $C_{\hat{\Gamma}, \pi/2}^P$ is the constant associated with the basic simplex $\hat{T}_{\pi/2}$ based on $\hat{A} = (0, 0)$, $\hat{B} = (1, 0)$, and $\hat{C} = (0, 1)$. Note that

$$\|\hat{w}\|_{\hat{T}_{\pi/2}}^2 = \frac{1}{\rho h^2 \sin \alpha} \|w\|_T^2, \quad (17)$$

and

$$\|\nabla \hat{w}\|_{\hat{T}_{\pi/2}}^2 \leq \frac{1}{\rho h^2 \sin \alpha} \int_T A_{\pi/2}(h, \rho, \alpha) \nabla w \cdot \nabla w \, dx, \quad (18)$$

where

$$A_{\pi/2}(h, \rho, \alpha) = h^2 \begin{pmatrix} 1 + \rho^2 \cos^2 \alpha & \rho^2 \sin \alpha \cos \alpha \\ \rho^2 \sin \alpha \cos \alpha & \rho^2 \sin^2 \alpha \end{pmatrix}.$$

It is not difficult to see that $\lambda_{\max}(A_{\pi/2}) = h^2 \mu_{\pi/2}(\rho, \alpha)$, where $\mu_{\pi/2}(\rho, \alpha)$ is defined in (13). From (16), (17), and (18), it follows that

$$\|w\|_T \leq \gamma_{\pi/2}^P C_{\hat{\Gamma}, \pi/2}^P h \|\nabla w\|_T, \quad \gamma_{\pi/2}^P(\rho, \alpha) = \mu_{\pi/2}^{1/2}(\rho, \alpha). \quad (19)$$

Notice that $\hat{w} \in \tilde{H}^1(\hat{T}, \hat{\Gamma})$ yields

$$\{w\}_{\Gamma} := \int_{\Gamma} w(x) \, ds = h \int_{\hat{\Gamma}} w(x(\hat{x})) \, d\hat{s} = h \int_{\hat{\Gamma}} \hat{w} \, d\hat{s} = 0.$$

Therefore, above mapping keeps $w \in \tilde{H}^1(T, \Gamma)$.

In view of inequality (4), for any $\hat{w} \in \tilde{H}^1(\hat{T}_{\pi/2}, \hat{\Gamma})$ we have

$$\|\hat{w}\|_{\hat{\Gamma}} \leq C_{\hat{\Gamma}, \pi/2}^{\text{Tr}} \|\nabla \hat{w}\|_{\hat{T}_{\pi/2}},$$

where $C_{\hat{\Gamma}, \pi/2}^{\text{Tr}}$ is the constant associated with the reference simplex $\hat{T}_{\pi/2}$. Since

$$\|\hat{w}\|_{\hat{\Gamma}}^2 = \frac{1}{h} \|w\|_{\Gamma}^2,$$

we obtain

$$\|w\|_{\Gamma} \leq \gamma_{\pi/2}^{\text{Tr}} C_{\hat{\Gamma}, \pi/2}^{\text{Tr}} h^{1/2} \|\nabla w\|_T, \quad \gamma_{\pi/2}^{\text{Tr}}(\rho, \alpha) = \left(\frac{\mu_{\pi/2}(\rho, \alpha)}{\rho \sin \alpha} \right)^{1/2}. \quad (20)$$

Now, we consider the mapping $\mathcal{F}_{\pi/4} : \hat{T}_{\pi/4} \rightarrow T$, where $\hat{T}_{\pi/4}$ is based on $\hat{A} = (0, 0)$, $\hat{B} = (1, 0)$, and $\hat{C} = (\frac{1}{2}, \frac{1}{2})$, i.e.,

$$x = \mathcal{F}_{\pi/4}(\hat{x}) = B_{\pi/4} \hat{x}, \quad \text{where } B_{\pi/4} = \begin{pmatrix} h & 2\rho h \cos \alpha - h \\ 0 & 2\rho h \sin \alpha \end{pmatrix}, \quad \det B_{\pi/4} = 2\rho h^2 \sin \alpha,$$

which yields another pair of estimates for the functions in $\tilde{H}^1(T, \Gamma)$:

$$\|w\|_T \leq \gamma_{\pi/4}^P C_{\hat{\Gamma}, \pi/4}^P h \|\nabla w\|_T, \quad \gamma_{\pi/4}^P(\rho, \alpha) = \mu_{\pi/4}^{1/2}(\rho, \alpha), \quad (21)$$

and

$$\|w\|_\Gamma \leq \gamma_{\pi/4}^{\text{Tr}} C_{\hat{\Gamma}, \pi/4}^{\text{Tr}} h^{1/2} \|\nabla w\|_T, \quad \gamma_{\pi/4}^{\text{Tr}}(\rho, \alpha) = \left(\frac{\mu_{\pi/4}(\rho, \alpha)}{2\rho \sin \alpha} \right)^{1/2}, \quad (22)$$

where $\mu_{\pi/4}(\rho, \alpha)$ is defined in (14). Now, (12) follows from (19), (20), (21), and (22). \square

Analogously to Lemma 1, one can obtain an upper bound of the constant in (1). For that we consider three reference triangles $\hat{T}_{\pi/2}$, $\hat{T}_{\pi/4}$ (defined earlier), and $\hat{T}_{\pi/3}$ based on vertexes $A = (0, 0)$, $B = (1, 0)$, $C = (\frac{1}{2}, \frac{\sqrt{3}}{2})$.

Lemma 2 For any $w \in \tilde{H}^1(T)$, the constant in

$$\|w\|_T \leq C_\Omega^P h \|\nabla w\|_T, \quad (23)$$

is estimated as

$$C_\Omega^P \leq \bar{C}_T^P = \min \left\{ \chi_{\pi/4}^P C_{\hat{T}, \pi/4}^P, \chi_{\pi/3}^P C_{\hat{T}, \pi/3}^P, \chi_{\pi/2}^P C_{\hat{T}, \pi/2}^P \right\}. \quad (24)$$

Here, $\chi_{\pi/4}^P = \mu_{\pi/4}^{1/2}$, $\chi_{\pi/3}^P = \mu_{\pi/3}^{1/2}$, $\chi_{\pi/2}^P = \mu_{\pi/2}^{1/2}$, where $\mu_{\pi/2}$ and $\mu_{\pi/4}$ being defined in (13) and (14), respectively, and

$$\mu_{\pi/3}(\rho, \alpha) = \frac{2}{3}(1 + \rho^2 - \rho \cos \alpha) + 2\left(\frac{1}{9}(1 + \rho^2 - \rho \cos \alpha)^2 - \frac{1}{3}\rho^2 \sin^2 \alpha\right)^{1/2}, \quad (25)$$

and $C_{\hat{T}, \pi/4}^P = \frac{1}{\sqrt{2\pi}}$, $C_{\hat{T}, \pi/3}^P = \frac{3}{4\pi}$, and $C_{\hat{T}, \pi/2}^P = \frac{1}{\pi}$.

Proof: The mapping $\mathcal{F}_{\pi/2} : \hat{T}_{\pi/2} \rightarrow T$ coincides with (2) from Lemma 1. It is easy to see that $w \in \tilde{H}^1(T)$ provides that $\hat{w} \in \tilde{H}^1(\hat{T})$. The estimate

$$\|w\|_T \leq \chi_{\pi/2}^P C_{\hat{T}, \pi/2}^P h \|\nabla w\|_T, \quad \chi_{\pi/2}^P(\rho, \alpha) = \mu_{\pi/2}^{1/2}(\rho, \alpha) \quad (26)$$

is obtained by following steps of the previous proof. From analysis of mappings

$$x = \mathcal{F}_{\pi/3}(\hat{x}) = B_{\pi/3} \hat{x}, \quad \text{where } B_{\pi/3} = \begin{pmatrix} h & \frac{h}{\sqrt{3}}(2\rho \cos \alpha - 1) - h \\ 0 & \frac{2h}{\sqrt{3}}\rho \sin \alpha \end{pmatrix}, \quad \det B_{\pi/3} = \frac{2h^2}{\sqrt{3}} \sin \alpha > 0,$$

and

$$x = \mathcal{F}_{\pi/4}(\hat{x}) = B_{\pi/4} \hat{x}, \quad \text{where } B_{\pi/4} = \begin{pmatrix} h & 2\rho h \cos \alpha - h \\ 0 & 2\rho h \sin \alpha \end{pmatrix}, \quad \det B_{\pi/4} = 2\rho h^2 \sin \alpha > 0,$$

we obtain alternative estimates

$$\|w\|_T \leq \chi_{\pi/3}^P C_{\hat{T}, \pi/3}^P h \|\nabla w\|_T, \quad \chi_{\pi/3}^P(\rho, \alpha) = \mu_{\pi/3}^{1/2}(\rho, \alpha), \quad (27)$$

$$\|w\|_T \leq \chi_{\pi/4}^P C_{\hat{T}, \pi/4}^P h \|\nabla w\|_T, \quad \chi_{\pi/4}^P(\rho, \alpha) = \mu_{\pi/4}^{1/2}(\rho, \alpha), \quad (28)$$

where $\mu_{\pi/3}(\rho, \alpha)$ and $\mu_{\pi/4}(\rho, \alpha)$ are defined in (25) and (14), respectively. Therefore, (24) follows from combination of (26), (27), and (28). \square

3 Minorants of C_Γ^P and C_Γ^{Tr} for triangular domains

3.1 Two-sided bounds of C_Γ^P and C_Γ^{Tr}

Majorants of C_Γ^P and C_Γ^{Tr} provided by Lemma 1 should be compared with the corresponding minorants, which can be found by means of the Rayleigh quotients

$$\mathcal{R}_\Gamma^P[w] = \frac{\|\nabla w\|_T}{\|w - \{w\}_\Gamma\|_T} \quad \text{and} \quad \mathcal{R}_\Gamma^{\text{Tr}}[w] = \frac{\|\nabla w\|_T}{\|w - \{w\}_\Gamma\|_\Gamma}. \quad (29)$$

Lower bounds are obtained if the quotients are minimized on finite dimensional subspaces $V^N \subset H^1(T)$ formed by sufficiently representative collections of suitable test functions. For this purpose, we use either power or Fourier series and introduce the spaces

$$V_1^N := \text{span}\{x^i y^j\} \quad \text{and} \quad V_2^N := \text{span}\{\cos(\pi i x) \overline{\cos(\pi j y)}\},$$

where $i, j = 0, \dots, N$, $(i, j) \neq (0, 0)$ and

$$\dim V_1^N = \dim V_2^N = M(N) := (N + 1)^2 - 1.$$

The corresponding constants are denoted by $\underline{C}_\Gamma^{M,P}$ and $\underline{C}_\Gamma^{M,\text{Tr}}$, where M indicates on number of basis functions in auxiliary subspace used. Since V_1^N and V_2^N are limit dense in $H^1(T)$, the respective minorants tend to the exact constants as $M(N)$ tends to infinity.

We note that

$$\inf_{w \in H^1(T)} \mathcal{R}_\Gamma^P[w] = \inf_{w \in H^1(T)} \frac{\|\nabla w\|_T}{\|w - \{w\}_\Gamma\|_T} = \inf_{w \in \widehat{H}^1(T, \Gamma)} \frac{\|\nabla w\|_T}{\|w\|_T} = \frac{1}{C_\Gamma^P}. \quad (30)$$

Therefore, minimization of the first quotient in (29) on V_1^N or V_2^N yields a lower bound of C_Γ^P . For the quotient $\mathcal{R}_\Gamma^{\text{Tr}}[w]$, we apply similar arguments.

Numerical results presented below are obtained with the help of two different codes based on the MATLAB Symbolic Math Toolbox [40] and The FEniCS Project [24]. Table 1 demonstrates the ratios between the exact constants and respective approximate values (for the selected ρ and α). They are quite close to 1 even for relatively small N . Henceforth, we select $N = 6$ or 7 in the tests discussed below.

		$\alpha = \frac{\pi}{2}, \rho = 1$		$\alpha = \frac{\pi}{4}, \rho = \frac{\sqrt{2}}{2}$	
N	$M(N)$	$\underline{C}_\Gamma^{M,P} / C_{\widehat{\Gamma}, \pi/2}^P$	$\underline{C}_\Gamma^{M,\text{Tr}} / C_{\widehat{\Gamma}, \pi/2}^{\text{Tr}}$	$\underline{C}_\Gamma^{M,P} / C_{\widehat{\Gamma}, \pi/4}^P$	$\underline{C}_\Gamma^{M,\text{Tr}} / C_{\widehat{\Gamma}, \pi/4}^{\text{Tr}}$
1	3	0.8801	0.9561	0.8647	1.0000
2	8	0.9945	0.9898	0.9925	1.0000
3	15	0.9999	0.9998	0.9962	1.0000
4	24	1.0000	0.9999	1.0000	1.0000
5	35	1.0000	1.0000	1.0000	1.0000
6	48	1.0000	1.0000	1.0000	1.0000

Table 1: Ratios between approximate and reference constants with respect to increasing N .

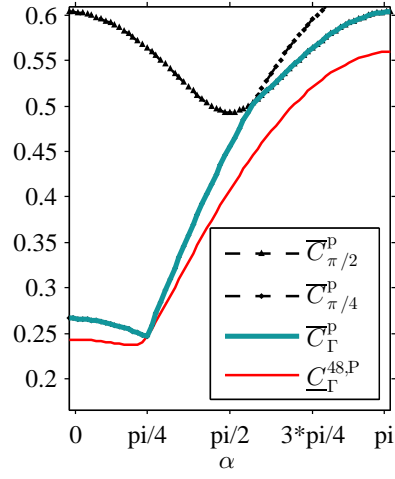
In Figs. 2a and 2c, we depict $\underline{C}_\Gamma^{M,P}$ for $M(N) = 48$ (thin red line) for T with $\rho = \frac{\sqrt{2}}{2}, 1$, and $\alpha \in (0, \pi)$. Guaranteed upper bounds $\overline{C}_{\pi/2}^P = \gamma_{\pi/2}^P C_{\widehat{\Gamma}, \pi/2}^P$ and $\overline{C}_{\pi/4}^P = \gamma_{\pi/4}^P C_{\widehat{\Gamma}, \pi/4}^P$ are depicted by dashed black lines. Bold blue line illustrates $\overline{C}_\Gamma^P = \min\{\overline{C}_{\pi/2}^P, \overline{C}_{\pi/4}^P\}$. Analogously in Figs. 3a and 3b, a red marker denotes the lower bound $\underline{C}_\Gamma^{M,\text{Tr}}$ (for $M(N) = 48$) of the constant C_Γ^{Tr} . It is presented together with the upper bound $\overline{C}_\Gamma^{\text{Tr}}$ (blue marker), which is defined as minimum of $\overline{C}_{\pi/2}^{\text{Tr}} = \gamma_{\pi/2}^{\text{Tr}} C_{\widehat{\Gamma}, \pi/2}^{\text{Tr}}$ and $\overline{C}_{\pi/4}^{\text{Tr}} = \gamma_{\pi/4}^{\text{Tr}} C_{\widehat{\Gamma}, \pi/4}^{\text{Tr}}$. Table 2 represents this information in the digital form.

Fig. 2a corresponds to the case $\rho = \frac{\sqrt{2}}{2}$. Notice that for $\alpha = \frac{\pi}{4}$ the constant C_Γ^P is known and the computed lower bound $\underline{C}_\Gamma^{M,P}$ (red marker) practically coincides with it (see, e.g., Fig. 2b). Since in this case, the mapping $\mathcal{F}_{\pi/4}$ is identical, the upper bound also coincides with the exact value. An analogous coincidence can be observed for C_Γ^{Tr} and $\underline{C}_\Gamma^{M,\text{Tr}}$ in Fig. 3a. In Fig. 2c, the red curve, corresponding to $\underline{C}_\Gamma^{M,P}$, coincides with the blue line of C_Γ^P at the point $\alpha = \frac{\pi}{2}$ (due to the fact that for this angle \mathcal{F} is the identical mapping and T coincides with $\widehat{T}_{\pi/2}$ (see Fig. 2d)). Fig. 3b exposes similar results for $\underline{C}_\Gamma^{M,\text{Tr}}$ and C_Γ^{Tr} ($\overline{C}_{\pi/2}^{\text{Tr}}$).

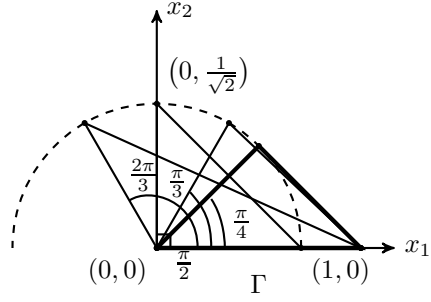
Figs. 4 and 5 demonstrate the same bounds for $\rho = \frac{\sqrt{3}}{2}$ and $\frac{3}{2}$. We see that estimates of C_Γ^P and C_Γ^{Tr} are very efficient. Namely, $I_{\text{eff}}^P := \frac{\overline{C}_\Gamma^P}{C_{48}^P} \in [1.0463, 1.1300]$ for $\rho = \frac{\sqrt{3}}{2}$ and $I_{\text{eff}}^P \in [1.0249, 1.1634]$ for $\rho = \frac{3}{2}$. Analogously, $I_{\text{eff}}^{\text{Tr}} := \frac{\overline{C}_\Gamma^{\text{Tr}}}{C_{48}^{\text{Tr}}} \in [1.0363, 1.3388]$ for $\rho = \frac{\sqrt{3}}{2}$ and $I_{\text{eff}}^{\text{Tr}} \in [1.2917, 1.7643]$ for $\rho = \frac{3}{2}$.

3.2 Two-sided bounds of C_T^P

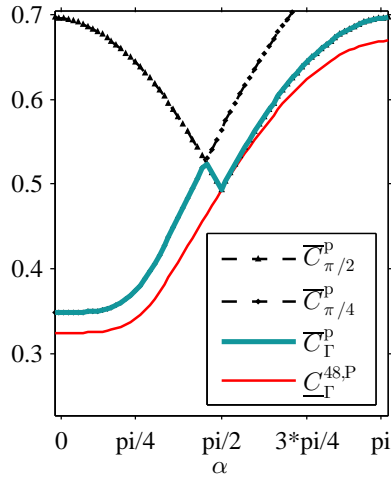
The spaces V_1^N and V_2^N can also be used for analysis of the quotient $\mathcal{R}_T[w] = \frac{\|\nabla w\|_T}{\|w - \{w\}_T\|_T}$, which yields guaranteed lower bounds of the constant in (1). The respective values are denoted by $\underline{C}_T^{M,P}$. These bounds are compared with $\overline{C}_T^{P,\oplus} := \frac{\text{diam}(T)}{j_{1,1}}$ and $\underline{C}_T^P := \max\left\{\frac{\text{diam}(T)}{2j_{0,1}}, \frac{P}{4\pi}\right\}$ (see (7)–(8), respectively) as well as the one derived in Lemma 2.



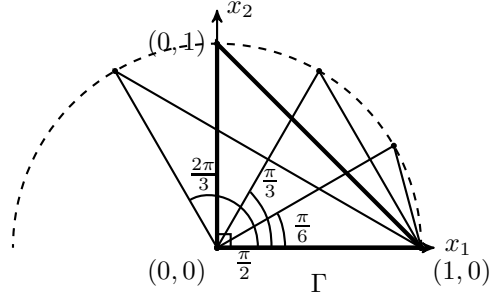
(a) $\rho = \frac{\sqrt{2}}{2}$



(b) $\rho = \frac{\sqrt{2}}{2}$

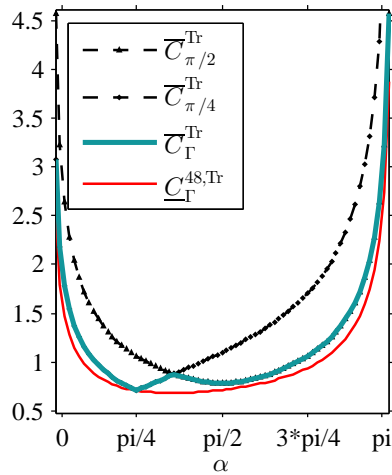


(c) $\rho = 1$

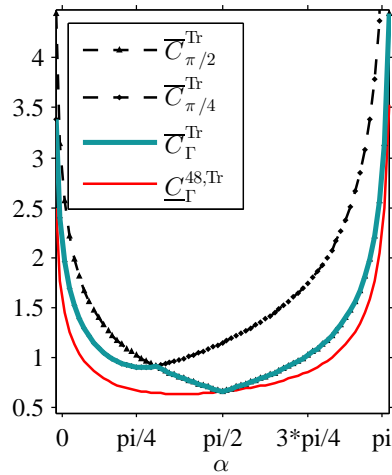


(d) $\rho = 1$

Figure 2: Two-sided bounds of C_Γ^P for T with different ρ .



(a) $\rho = \frac{\sqrt{2}}{2}$



(b) $\rho = 1$

Figure 3: Two-sided bounds of C_Γ^{Tr} for T with different ρ .

α	$\rho = \frac{\sqrt{2}}{2}$				$\rho = 1$			
	$\underline{C}_\Gamma^{48,P}$	\overline{C}_Γ^P	$\underline{C}_\Gamma^{48,Tr}$	\overline{C}_Γ^{Tr}	$\underline{C}_\Gamma^{48,P}$	\overline{C}_Γ^P	$\underline{C}_\Gamma^{48,Tr}$	\overline{C}_Γ^{Tr}
$\pi/18$	0.2429	0.2657	1.2786	1.5386	0.3245	0.3486	1.2572	1.6971
$\pi/9$	0.2414	0.2627	0.9289	1.0838	0.3248	0.3493	0.9058	1.2116
$\pi/6$	0.2389	0.2577	0.7919	0.8792	0.3268	0.3527	0.7632	1.0118
$2\pi/9$	0.2379	0.2507	0.7259	0.7543	0.3339	0.3636	0.6906	0.9201
$5\pi/18$	0.2632	0.2722	0.6945	0.7503	0.3514	0.3884	0.6529	0.9003
$\pi/3$	0.3008	0.3220	0.6829	0.8348	0.3809	0.4269	0.6362	0.8634
$7\pi/18$	0.3382	0.3694	0.6840	0.8432	0.4173	0.4721	0.6332	0.7840
$4\pi/9$	0.3740	0.4140	0.6947	0.7973	0.4556	0.5187	0.6404	0.7162
$\pi/2$	0.4075	0.4554	0.7136	0.7801	0.4929	0.4929	0.6560	0.6560
$5\pi/9$	0.4382	0.4933	0.7409	0.7973	0.5280	0.5340	0.6797	0.7162
$11\pi/18$	0.4660	0.5165	0.7779	0.8432	0.5600	0.5710	0.7125	0.7840
$2\pi/3$	0.4905	0.5361	0.8274	0.9118	0.5884	0.6037	0.7569	0.8634
$13\pi/18$	0.5115	0.5552	0.8948	1.0040	0.6129	0.6318	0.8175	0.9607
$7\pi/9$	0.5289	0.5720	0.9898	1.1292	0.6332	0.6550	0.9033	1.0874
$5\pi/6$	0.5426	0.5856	1.1334	1.3107	0.6492	0.6733	1.0332	1.2673
$8\pi/9$	0.5524	0.5956	1.3796	1.6118	0.6607	0.6865	1.2565	1.5623
$17\pi/18$	0.5583	0.6017	1.9436	2.2851	0.6676	0.6944	1.7692	2.2179

Table 2: Two-sided bounds of C_Γ^P and C_Γ^{Tr} for T for $\alpha \in (0, \pi)$ and different ρ .

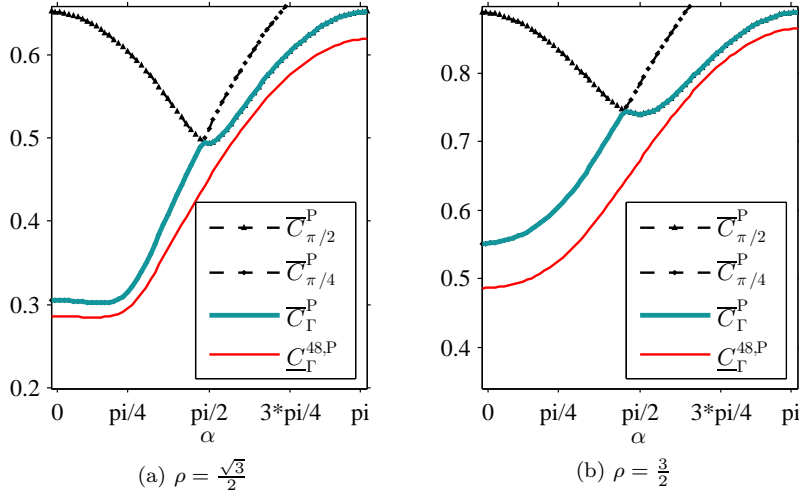


Figure 4: Two-sided bounds of C_Γ^P for T with different ρ .

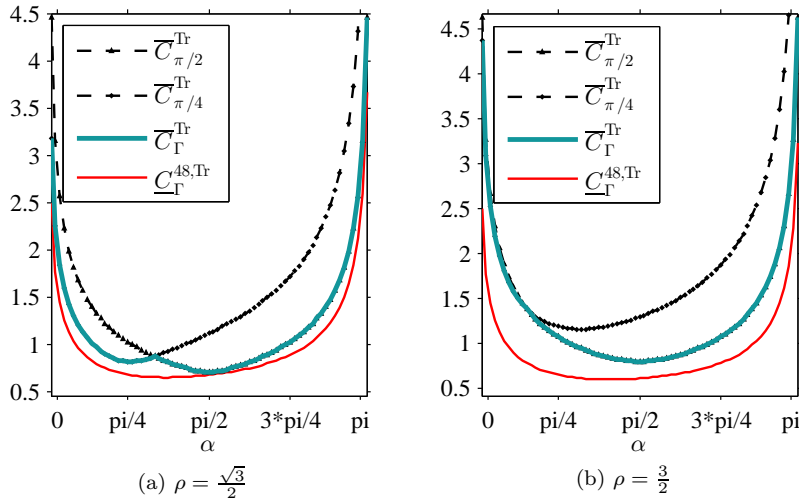


Figure 5: Two-sided bounds of C_Γ^{Tr} for T with different ρ .

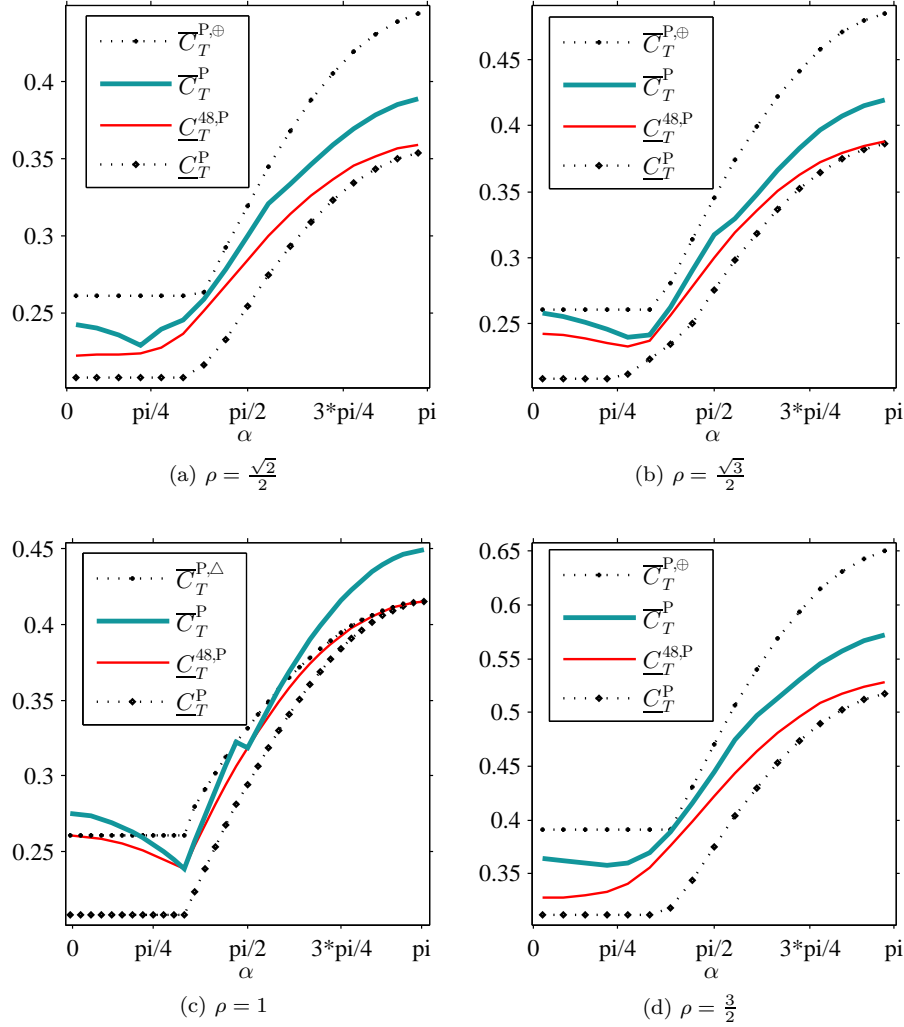


Figure 6: \underline{C}_T^{48} , $\overline{C}_T^{P,\Delta}$, \overline{C}_T^P , and \underline{C}_T^P for T with $\alpha \in (0, \pi)$ and different ρ .

In Figs. 6a, 6b, and 6d, we present $\underline{C}_T^{M,P}$ (in this case $M(N) = 48$) together with \overline{C}_T^P (blue thick line), $\overline{C}_T^{P,\oplus}$ and \underline{C}_T^P for $\alpha \in (0, \pi)$, and $\rho = \frac{\sqrt{2}}{2}$, $\frac{\sqrt{3}}{2}$, and $\frac{3}{2}$. We see that $\underline{C}_T^{48,P}$ (red thin line) indeed lies within the admissible two-sided bounds. From these figures, it is obvious that new upper bounds \overline{C}_T^P are sharper than $\overline{C}_T^{P,\oplus}$ for T with $\rho \neq 1$. True values of the constant lie between the bold blue and thin red lines, but closer to the red one, which practically shows the constant (this follows from the fact that increasing $M(N)$ does not provide a noticeable change for the line, e.g., for $M(N) = 63$ maximal difference with respect to figure does not exceed $1e-8$). Also, we note that, the lower bound \underline{C}_T^P (black dashed line) is quite efficient, and, moreover, asymptotically exact for $\alpha \rightarrow \pi$.

Due to [22] and [3], we know the improved upper bound $\overline{C}_T^{P,\Delta}$ (cf. (6)) for isosceles triangles. In Fig. 6c, we compare $\underline{C}_T^{M,P}$ ($M(N) = 48$) with both upper bounds \overline{C}_T^P (from the Lemma 2) and $\overline{C}_T^{P,\Delta}$ (black dotted line). It is easy to see that $\overline{C}_T^{P,\Delta}$ (black dashed line) is rather accurate and for $\alpha \rightarrow 0$ and $\alpha \rightarrow \pi$ provide almost exact estimates. \overline{C}_T^P (blues thick line) improves $\overline{C}_T^{P,\Delta}$ only for some α . The lower bound \underline{C}_T^{48} (red thin line) indeed converges to $\overline{C}_T^{P,\Delta}$ as T degenerates when α tends to 0.

3.3 Shape of the minimizer

Exact constants in (2) and (4) are generated by the minimal positive eigenvalues of (3) and (5). This section presents results related to the respective eigenfunctions. In order to depict all of them in a unified form, we use the barycentric coordinates $\lambda_i \in (0, 1)$, $i = 1, 2, 3$, $\sum_{i=1}^3 \lambda_i = 1$.

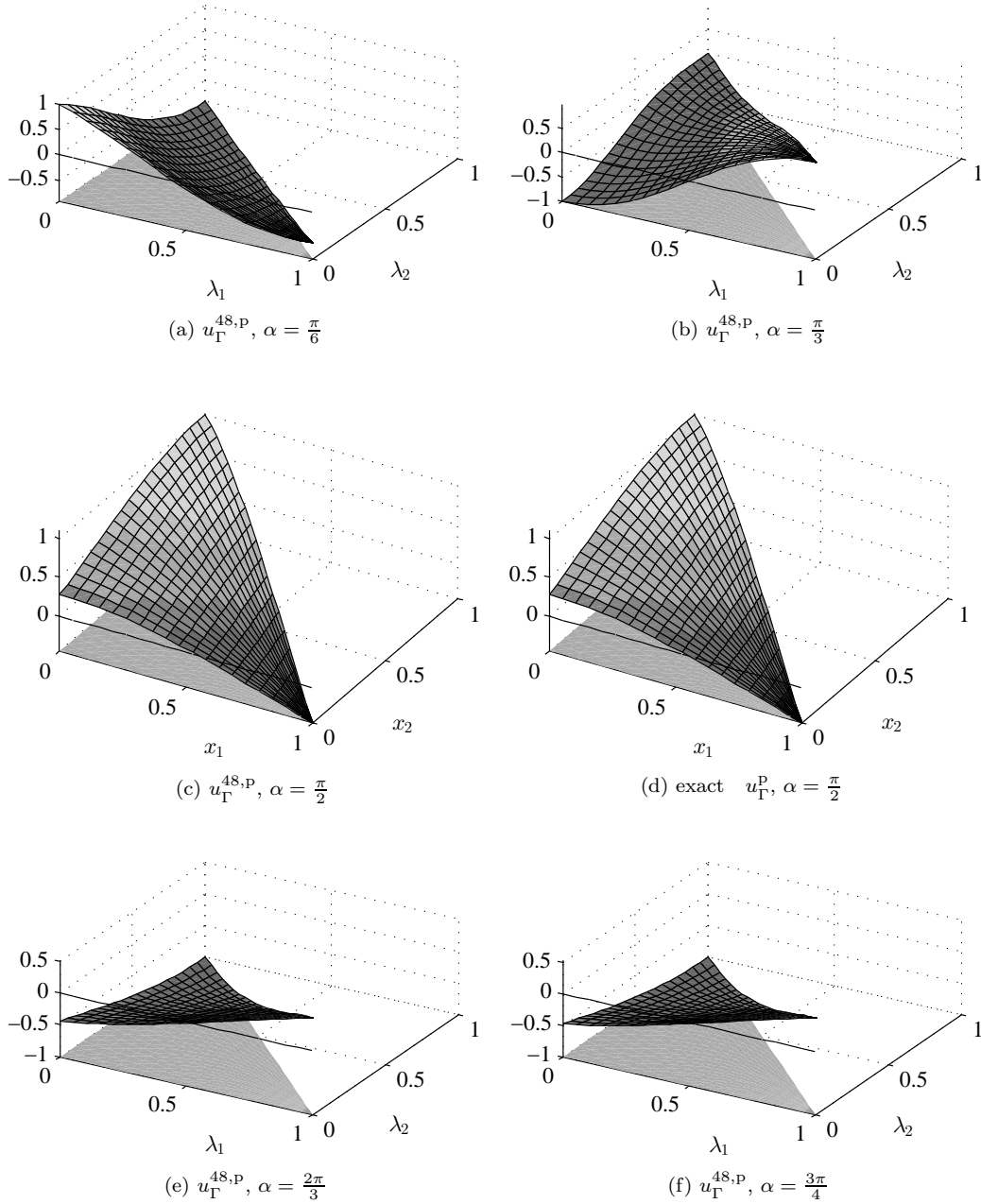


Figure 7: Eigenfunctions corresponding to $\underline{C}_\Gamma^{M,P}$ and for $M = 48$ on simplex T with $\rho = 1$ and different α .

Figs. 7 and 8 show the eigenfunctions computed for isosceles triangles with different angles α between two legs (zero mean condition is imposed on one of the legs). The eigenfunctions have been computed in the process of finding $\underline{C}_\Gamma^{M,P}$ and $\underline{C}_\Gamma^{M,\text{Tr}}$. The eigenfunctions are normalized so that the maximal value is equal to 1. For $\alpha = \frac{\pi}{2}$, the exact eigenfunction associated with the smallest positive eigenvalue $\lambda_\Gamma^P = \left(\frac{\zeta_0}{h}\right)^2$ is known (see [29]):

$$u_\Gamma^P = \cos\left(\frac{\zeta_0 x_1}{h}\right) + \cos\left(\frac{\zeta_0(x_2 - h)}{h}\right).$$

Here, ζ_0 is the root of the first equation in (10) (see Fig 7d). We can compare u_Γ^P with the approximate eigenfunction $u_\Gamma^{M,P}$ computed by minimization of $\mathcal{R}_\Gamma^P[w]$ (this function is depicted in Fig. 7c).

Eigenfunctions related to the constant $\underline{C}_\Gamma^{M,\text{Tr}}$ are presented in Fig. 8. Again, for $\alpha = \frac{\pi}{2}$ we know the exact eigenfunction

$$u_\Gamma^{\text{Tr}} = \cos(\hat{\zeta}_0 x_1) \cosh(\hat{\zeta}_0(x_2 - h)) + \cosh(\hat{\zeta}_0 x_1) \cos(\hat{\zeta}_0(x_2 - h)),$$

where $\hat{\zeta}_0$ is the root of second equation in (10) (see Fig. 8d). This function minimizes the quotient $\mathcal{R}_\Gamma^{\text{Tr}}[w]$ and

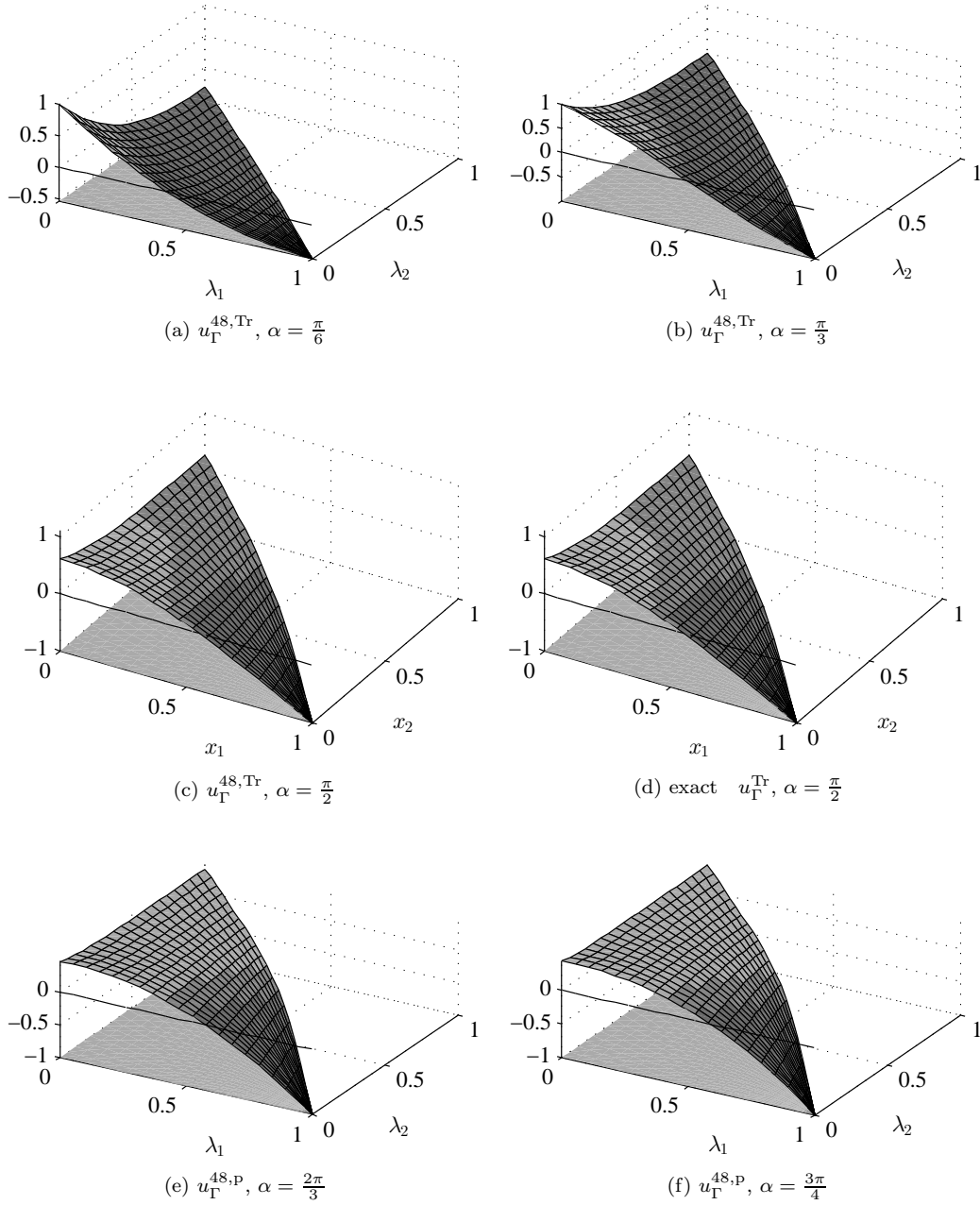


Figure 8: Eigenfunctions corresponding to $\underline{C}_\Gamma^{M,\text{Tr}}$ for $M = 48$ on simplex T with $\rho = 1$ and different α .

yields the smallest positive eigenvalue $\lambda_\Gamma^{\text{Tr}} = \frac{\hat{\zeta}_0 \tanh(\hat{\zeta}_0)}{h}$. It is easy to see that numerical approximation $\underline{C}_\Gamma^{M,\text{Tr}}$ (for $M(N) = 48$) practically coincides with the exact function.

Typically, the eigenfunctions associated with minimal positive eigenvalues expose a continuous evolution with respect to α . However, this is not true for the quotient $\mathcal{R}_T[w]$, where the minimizer radically changes the profile. Fig. 6c indicates a possibility of such a rapid change at $\alpha = \frac{\pi}{3}$, where the curve (related to \underline{C}_T^{48}) obviously becomes non-smooth. This happens because an equilateral triangle has double eigenvalue, therefore the minimizer of $\mathcal{R}_T[w]$ over V_1^N changes its profile. Figs. 9a–9i show three eigenfunctions $u_{T,1}^{48}$, $u_{T,2}^{48}$, and $u_{T,3}^{48}$ corresponding to three minimal eigenvalues $\lambda_{T,1}^{48}$, $\lambda_{T,2}^{48}$, and $\lambda_{T,3}^{48}$. All functions are computed for isosceles triangles and are sorted in accordance with increasing values of the respective eigenvalues. It is easy to see that at $\alpha = \frac{\pi}{3}$ the first and the second eigenfunctions swap places. Table 3 presents the corresponding results in the digital form.

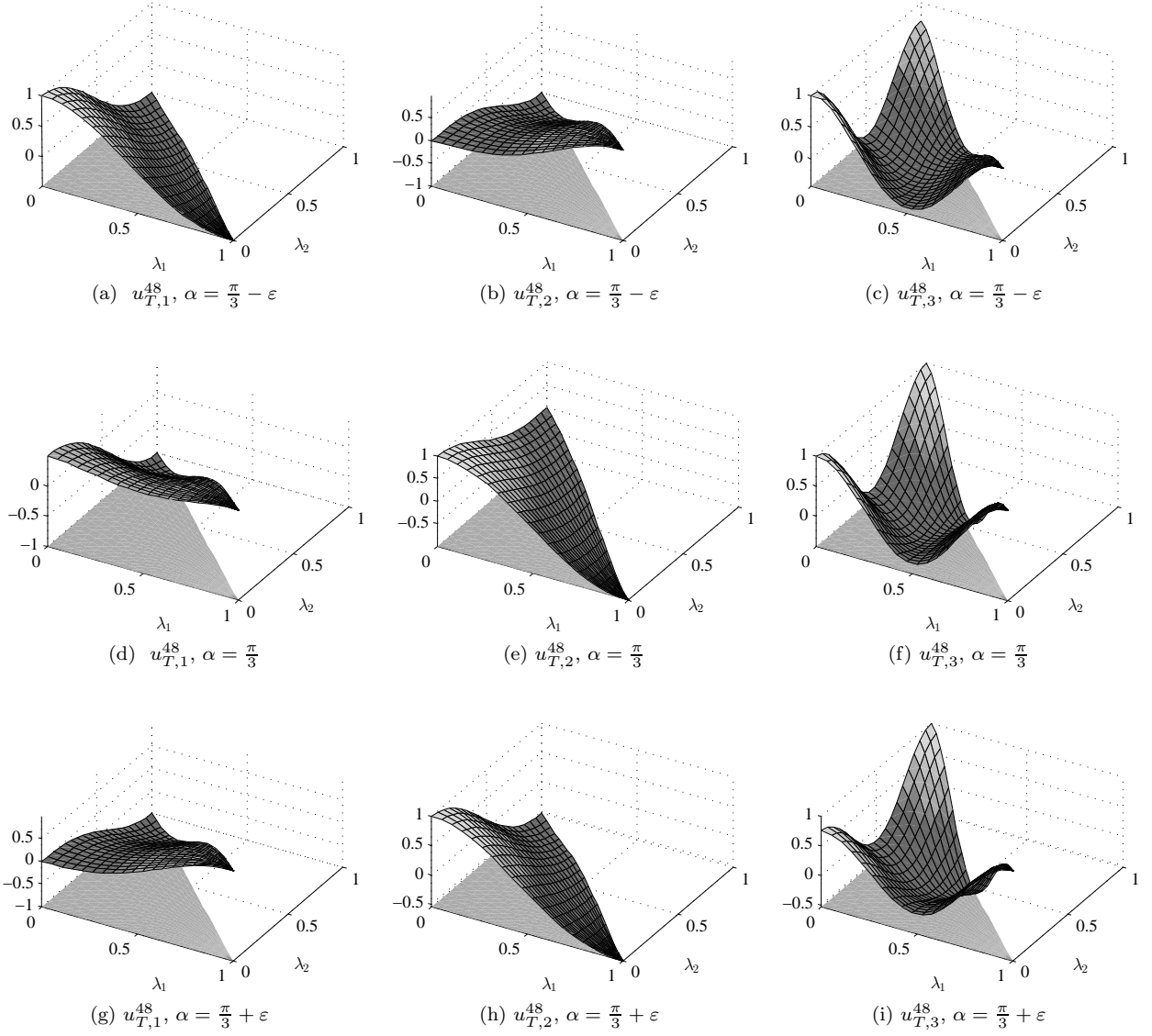


Figure 9: Eigenfunctions corresponding to $\underline{C}_T^{M,P}$ with $M = 48$ on isosceles triangles $T \in \mathbb{R}^2$ with $\alpha = \frac{\pi}{3}, \frac{\pi}{3} - \varepsilon$, and $\frac{\pi}{3} + \varepsilon$ in barycentric coordinates.

		$\frac{\pi}{3} - \varepsilon$		$\frac{\pi}{3}$		$\frac{\pi}{3} + \varepsilon$	
	$u_{T,i}^M$	$\underline{C}_{T,i}^{48}$	$\lambda_{T,i}^{48}$	$\underline{C}_{T,i}^{48}$	$\lambda_{T,i}^{48}$	$\underline{C}_{T,i}^{48}$	$\lambda_{T,i}^{48}$
$\rho = 1$	$u_{T,1}^{48}$	0.2419	17.0951	0.2387	17.5463	0.2537	15.5404
	$u_{T,2}^{48}$	0.2229	20.1216	0.2387	17.5463	0.2355	18.0309
	$u_{T,3}^{48}$	0.1353	54.6024	0.1378	52.6396	0.1422	49.4818
$\rho = \frac{\sqrt{2}}{2}$	$u_{T,1}^{48}$	0.23137	18.6804	0.23671	17.8471	0.24336	16.8850
	$u_{T,2}^{48}$	0.17082	34.2707	0.17435	32.8970	0.17642	32.1295
	$u_{T,3}^{48}$	0.1229	66.2058	0.12789	61.1402	0.13298	56.5493
$\rho = \frac{3}{2}$	$u_{T,1}^{48}$	0.34714	8.2983	0.35523	7.9247	0.3648	7.5143
	$u_{T,2}^{48}$	0.24485	16.6801	0.24885	16.1482	0.25125	15.8412
	$u_{T,3}^{48}$	0.18258	29.9981	0.19084	27.4575	0.19845	25.3921

Table 3: $\underline{C}_T^{M,P}$ and λ_T^M corresponding to the first three eigenfunctions in Fig. 9.

It is worth noting that for equilateral triangles two minimal eigenfunctions are known (see [26]):

$$\begin{aligned}
 u_1 &= \cos\left(\frac{2\pi}{3}(2x_1 - 1)\right) - \cos\left(\frac{2\pi}{\sqrt{3}}x_2\right) \cos\left(\frac{\pi}{3}(2x_1 - 1)\right), \\
 u_2 &= \sin\left(\frac{2\pi}{3}(2x_1 - 1)\right) + \cos\left(\frac{2\pi}{\sqrt{3}}x_2\right) \sin\left(\frac{\pi}{3}(2x_1 - 1)\right).
 \end{aligned}$$

	$\hat{\alpha} = \frac{\pi}{4}$	$\hat{\alpha} = \frac{\pi}{3}$	$\hat{\alpha} = \frac{\pi}{2}$	$\hat{\alpha} = \frac{2\pi}{3}$				
$M(N)$	$C_{\hat{\Gamma}, \pi/2, \hat{\alpha}}^{P, M}$	$C_{\hat{\Gamma}, \pi/2, \hat{\alpha}}^{\text{Tr}, M}$	$C_{\hat{\Gamma}, \pi/2, \hat{\alpha}}^{P, M}$	$C_{\hat{\Gamma}, \pi/2, \hat{\alpha}}^{\text{Tr}, M}$	$C_{\hat{\Gamma}, \pi/2, \hat{\alpha}}^{P, M}$	$C_{\hat{\Gamma}, \pi/2, \hat{\alpha}}^{\text{Tr}, M}$	$C_{\hat{\Gamma}, \pi/2, \hat{\alpha}}^{P, M}$	$C_{\hat{\Gamma}, \pi/2, \hat{\alpha}}^{\text{Tr}, M}$
7	0.32431	0.760099	0.325985	0.654654	0.360532	0.654654	0.4152099	0.686161
26	0.338539	0.829445	0.340267	0.761278	0.373669	0.751615	0.4274757	0.863324
63	0.341122	0.831325	0.342556	0.762901	0.375590	0.751994	0.4286444	0.864595
124	0.341147	0.831335	0.342589	0.762905	0.375603	0.751999	0.4286652	0.864630
215	0.341147	0.831335	0.342589	0.762905	0.375603	0.751999	0.4286652	0.864630

Table 4: $C_{\hat{\Gamma}, \pi/2, \hat{\alpha}}^{P, M}$ and $C_{\hat{\Gamma}, \pi/2, \hat{\alpha}}^{\text{Tr}, M}$ with respect to $M(N)$ for $\hat{T}_{\hat{\theta}, \hat{\alpha}}$ with $\rho = 1$, $\hat{\theta} = \frac{\pi}{2}$, and different $\hat{\alpha}$.

These functions practically coincide with the functions $u_{T,1}^{48}$ and $u_{T,2}^{48}$ presented in Fig. 9d. Finally, we note that this phenomenon (change of the minimal eigenfunction) does not appear for $\rho = \frac{\sqrt{2}}{2}$ or $\rho = \frac{3}{2}$. The eigenvalues as well as the constants corresponding to the eigenfunctions presented in Fig. 9 are shown in the Table 3.

4 Two-sided bounds of C_{Γ}^P and C_{Γ}^{Tr} for tetrahedrons

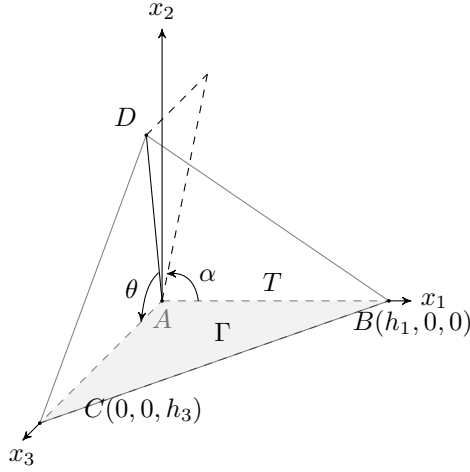


Figure 10: Simplex in \mathbb{R}^3 .

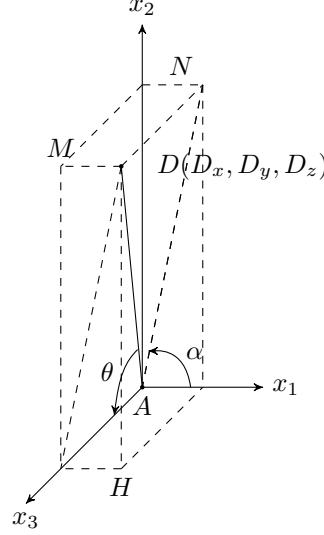


Figure 11: Coordinate of the vertex D .

We orient the coordinates as it is shown in Fig. 10 and define a non-degenerate simplex in \mathbb{R}^3 with vertexes $A = (0, 0, 0)$, $B = (h_1, 0, 0)$, $C = (0, 0, h_3)$, and $D = (h_2 \sin \theta \cos \alpha, h_2 \sin \theta \sin \alpha, h_2 \cos \alpha)$, where h_1 and h_3 are the scaling parameters along axis O_{x_1} and O_{x_3} , respectively, $AD = h_2$, α is a polar angle, and θ is an azimuthal angle (see Fig. 11). Let Γ be defined by vertexes A , B , and C .

To the best of our knowledge, exact values of constants in Poincaré-type inequalities for simplexes in \mathbb{R}^3 are unknown. Therefore, we first consider four basic (reference) tetrahedrons with $h_2 = 1$, $\hat{\theta} = \frac{\pi}{2}$, and $\hat{\alpha}_1 = \frac{\pi}{4}$, $\hat{\alpha}_2 = \frac{\pi}{3}$, $\hat{\alpha}_3 = \frac{\pi}{2}$, and $\hat{\alpha}_4 = \frac{2\pi}{3}$. The respective constants are found numerically with high accuracy (see Table 4, which shows convergence of the constants with respect to increasing $M(N)$). Henceforth, $\hat{T}_{\hat{\theta}, \hat{\alpha}}$ denotes a reference tetrahedron, where $\hat{\theta}$ and $\hat{\alpha}$ are certain fixed angles. By $\mathcal{F}_{\hat{\theta}, \hat{\alpha}}$ we denote the respective mapping $\mathcal{F}_{\hat{\theta}, \hat{\alpha}} : \hat{T}_{\hat{\theta}, \hat{\alpha}} \rightarrow T$. Then, for an arbitrary tetrahedron T , we have

$$\|v\|_T \leq C_{\Gamma}^P h_2 \|\nabla v\|_T \quad \text{and} \quad \|v\|_{\Gamma} \leq C_{\Gamma}^{\text{Tr}} h_2^{1/2} \|\nabla v\|_T \quad (31)$$

with approximate bounds

$$C_{\Gamma}^{\text{P}} \lesssim \tilde{C}_{\Gamma}^{\text{P}} = \min_{\hat{\alpha}=\{\pi/4, \pi/3, \pi/2, 2\pi/3\}} \left\{ \gamma_{\pi/2, \hat{\alpha}}^{\text{P}} C_{\Gamma, \pi/2, \hat{\alpha}}^{\text{P}} \right\} \quad (32)$$

and

$$C_{\Gamma}^{\text{Tr}} \lesssim \tilde{C}_{\Gamma}^{\text{Tr}} = \min_{\hat{\alpha}=\{\pi/4, \pi/3, \pi/2, 2\pi/3\}} \left\{ \gamma_{\pi/2, \hat{\alpha}}^{\text{Tr}} C_{\Gamma, \pi/2, \hat{\alpha}}^{\text{Tr}} \right\}, \quad (33)$$

where $C_{\Gamma, \pi/2, \hat{\alpha}}^{\text{P}}$ and $C_{\Gamma, \pi/2, \hat{\alpha}}^{\text{Tr}}$ are the constants related to four reference tetrahedrons from Table 4, and $\gamma_{\pi/2, \hat{\alpha}}^{\text{P}}$ and $\gamma_{\pi/2, \hat{\alpha}}^{\text{Tr}}$ (see (34)) are generated by the mapping $\mathcal{F}_{\pi/2, \hat{\alpha}}: \hat{T}_{\pi/2, \hat{\alpha}} \rightarrow T$. Here, the reference tetrahedrons are defined based on $\hat{A} = (0, 0, 0)$, $\hat{B} = (1, 0, 0)$, $\hat{C} = (0, 0, 1)$, $\hat{D} = (\cos \hat{\alpha}, \sin \hat{\alpha}, 0)$ with $\hat{\alpha} = \{\frac{\pi}{4}, \frac{\pi}{3}, \frac{\pi}{2}, \frac{2\pi}{3}\}$, and $\mathcal{F}_{\pi/2, \hat{\alpha}}(\hat{x})$ is presented by the relation

$$x = \mathcal{F}_{\pi/2, \hat{\alpha}}(\hat{x}) = B_{\pi/2, \hat{\alpha}} \hat{x}, \quad B_{\pi/2, \hat{\alpha}} = \{b_{ij}\}_{i,j=1,2,3} = h_2 \begin{pmatrix} \frac{h_1}{h_2} & \frac{\nu(\rho, \alpha)}{\sin \hat{\alpha}} & 0 \\ 0 & \frac{\sin \alpha \sin \theta}{\sin \hat{\alpha}} & 0 \\ 0 & \frac{\cos \theta}{\sin \hat{\alpha}} & \frac{h_3}{h_2} \end{pmatrix},$$

where $\nu(\rho, \alpha) = \cos \alpha \sin \theta - \frac{h_1}{h_2} \cos \hat{\alpha}$, $\det B_{\pi/2, \hat{\alpha}} = h_1 h_2 h_3 \frac{\sin \alpha \sin \theta}{\sin \hat{\alpha}}$. By analogy with the two-dimensional case (see (18)), $\gamma_{\pi/2, \hat{\alpha}}^{\text{P}}$ and $\gamma_{\pi/2, \hat{\alpha}}^{\text{Tr}}$ depend on the maximum eigenvalue of the matrix

$$A_{\pi/2, \hat{\alpha}} := h_1^2 \begin{pmatrix} b_{11}^2 + b_{12}^2 & b_{12}b_{22} & b_{12}b_{32} \\ b_{12}b_{22} & b_{22}^2 & b_{22}b_{32} \\ b_{12}b_{32} & b_{22}b_{32} & b_{33}^2 + b_{32}^2 \end{pmatrix}.$$

The maximal eigenvalue of the matrix $A_{\pi/2, \hat{\alpha}}$ is defined by the relation $\lambda_{\max}(A_{\pi/2, \hat{\alpha}}) = h_2^2 \mu_{\alpha, \theta, \hat{\alpha}}$ with

$$\mu_{\alpha, \theta, \hat{\alpha}} = \left(\mathcal{E}_5^{1/3} - \mathcal{E}_3 \mathcal{E}_5^{-1/3} + \frac{1}{3} \mathcal{E}_1 \right),$$

where

$$\begin{aligned} \mathcal{E}_1 &= b_{11}^2 + b_{12}^2 + b_{22}^2 + b_{32}^2 + b_{33}^2, \\ \mathcal{E}_2 &= b_{11}^2 b_{22}^2 + b_{11}^2 b_{32}^2 + b_{11}^2 b_{33}^2 + b_{12}^2 b_{33}^2 + b_{22}^2 b_{33}^2, \\ \mathcal{E}_3 &= \frac{\mathcal{E}_2}{3} - \left(\frac{\mathcal{E}_1}{3} \right)^2, \\ \mathcal{E}_4 &= \left(\frac{\mathcal{E}_1}{3} \right)^3 - \frac{\mathcal{E}_1 \mathcal{E}_2}{3} + \frac{1}{2} b_{11}^2 b_{22}^2 b_{33}^2, \\ \mathcal{E}_5 &= \mathcal{E}_4 + (\mathcal{E}_3^3 + \mathcal{E}_4^2)^{1/2}. \end{aligned}$$

Therefore, $\gamma_{\pi/2, \hat{\alpha}}^{\text{P}}$ and $\gamma_{\pi/2, \hat{\alpha}}^{\text{Tr}}$ in (31) are as follows:

$$\gamma_{\pi/2, \hat{\alpha}}^{\text{P}} = \mu_{\pi/2, \hat{\alpha}}^{1/2}, \quad \gamma_{\pi/2, \hat{\alpha}}^{\text{Tr}} = \left(\frac{\sin \hat{\alpha}}{\rho \sin \alpha \sin \theta} \right)^{1/2} \gamma_{\pi/2, \hat{\alpha}}^{\text{P}}. \quad (34)$$

Lower bounds of the constants C_{Γ}^{P} and C_{Γ}^{Tr} are computed by minimization of $\mathcal{R}_{\Gamma}^{\text{P}}[w]$ and $\mathcal{R}_{\Gamma}^{\text{Tr}}[w]$ over the set $V_3^N \subset H^1(T)$, where

$$V_3^N := \left\{ \varphi_{ijk} = x^i y^j z^k, \quad i, j, k = 0, \dots, N, \quad (i, j, k) \neq (0, 0, 0) \right\}$$

and $\dim V_3^N = M(N) := (N+1)^3 - 1$.

The respective results are presented in Tables 5 and 6 for T with $h_1 = 1$, $h_3 = 1$, and $\rho = 1$. We note that exact values of constants are probably closer to the numbers presented in left-hand side columns. For $\theta = \pi/2$, we also present estimates of $\underline{C}_{\Gamma}^{M, \text{P}}$ and $\underline{C}_{\Gamma}^{M, \text{Tr}}$ (red lines) graphically in Fig. 12.

5 Example

Constants in the Friedrichs', Poincaré, and other functional inequalities arise in various problems of numerical analysis, where we need to know values of the respective constants associated with particular domains. Constants in projection type estimates arise in a priori analysis (see, e.g., [6, 11, 27]). Constants in Clement's interpolation inequalities are important for residual type a posteriori estimates (see, e.g., [1, 42], and [7], where these constants have been evaluated). Concerning constants in the trace inequalities associated with polygonal domain, we mention

	$\alpha = \frac{\pi}{6}$		$\alpha = \frac{\pi}{4}$		$\alpha = \frac{\pi}{3}$		$\alpha = \frac{\pi}{2}$	
θ	$\underline{C}_\Gamma^{M,P}$	\tilde{C}_Γ^P	$\underline{C}_\Gamma^{M,P}$	\tilde{C}_Γ^P	$\underline{C}_\Gamma^{M,P}$	\tilde{C}_Γ^P	$\underline{C}_\Gamma^{M,P}$	\tilde{C}_Γ^P
$\pi/6$	0.23883	0.49035	0.24621	0.49841	0.25870	0.51054	0.29484	0.51308
$\pi/4$	0.23883	0.45388	0.24621	0.46173	0.25870	0.47683	0.29484	0.49075
$\pi/3$	0.29666	0.41958	0.31194	0.42259	0.33489	0.43724	0.38976	0.46002
$\pi/2$	0.34302	0.35667	0.34112	0.34115	0.34256	0.34259	0.37559	0.37560
$2\pi/3$	0.40428	0.41958	0.40562	0.42259	0.40927	0.43724	0.42867	0.46002
$3\pi/4$	0.42890	0.45388	0.43110	0.46173	0.43505	0.47683	0.45017	0.49075
$5\pi/6$	0.44964	0.49035	0.45193	0.49841	0.45539	0.51054	0.46607	0.51308
	$\alpha = \frac{\pi}{2}$		$\alpha = \frac{2\pi}{3}$		$\alpha = \frac{3\pi}{4}$		$\alpha = \frac{5\pi}{6}$	
θ	$\underline{C}_\Gamma^{M,P}$	\tilde{C}_Γ^P	$\underline{C}_\Gamma^{M,P}$	\tilde{C}_Γ^P	$\underline{C}_\Gamma^{M,P}$	\tilde{C}_Γ^P	$\underline{C}_\Gamma^{M,P}$	\tilde{C}_Γ^P
$\pi/6$	0.29484	0.51308	0.33069	0.51792	0.34468	0.52253	0.35499	0.52694
$\pi/4$	0.29484	0.49075	0.33069	0.50261	0.34468	0.51308	0.35499	0.52253
$\pi/3$	0.38976	0.46002	0.43880	0.48413	0.45742	0.50261	0.47106	0.51792
$\pi/2$	0.37559	0.37560	0.42865	0.42867	0.45017	0.45731	0.46607	0.47811
$2\pi/3$	0.42867	0.46002	0.45997	0.48413	0.47457	0.50261	0.48598	0.51792
$3\pi/4$	0.45017	0.49075	0.47204	0.50261	0.48239	0.51308	0.49064	0.52253
$5\pi/6$	0.46607	0.51308	0.47972	0.51792	0.48607	0.52253	0.49115	0.52694

Table 5: $\underline{C}_\Gamma^{M,P}$ ($M(N) = 124$) and \tilde{C}_Γ^P .

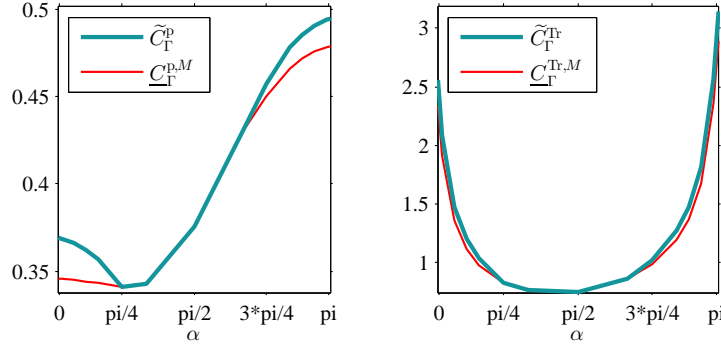


Figure 12: C_Γ^P and C_Γ^{Tr} for $T \in \mathbb{R}^3$ with $H = 1$, $\rho = 1$ with estimate based on four reference tetrahedrons.

	$\alpha = \frac{\pi}{6}$		$\alpha = \frac{\pi}{4}$		$\alpha = \frac{\pi}{3}$		$\alpha = \frac{\pi}{2}$	
θ	$\underline{C}_\Gamma^{M,\text{Tr}}$	$\tilde{C}_\Gamma^{\text{Tr}}$	$\underline{C}_\Gamma^{M,\text{Tr}}$	$\tilde{C}_\Gamma^{\text{Tr}}$	$\underline{C}_\Gamma^{M,\text{Tr}}$	$\tilde{C}_\Gamma^{\text{Tr}}$	$\underline{C}_\Gamma^{M,\text{Tr}}$	$\tilde{C}_\Gamma^{\text{Tr}}$
$\pi/6$	1.09760	3.78259	0.96245	2.71866	0.91255	2.27382	0.93123	2.05449
$\pi/4$	1.09760	2.43897	0.96245	1.78094	0.91255	1.50166	0.93123	1.38951
$\pi/3$	0.89122	1.74467	0.79146	1.31130	0.75950	1.12431	0.78904	1.06349
$\pi/2$	0.98017	1.22920	0.83132	0.83133	0.76290	0.76291	0.75199	0.75200
$2\pi/3$	1.17698	1.74467	0.99473	1.31130	0.90578	1.12431	0.86463	1.06349
$3\pi/4$	1.35195	2.43897	1.14144	1.78094	1.03737	1.50166	0.98220	1.38951
$5\pi/6$	1.65317	3.78259	1.39424	2.71866	1.26490	2.27382	1.19017	2.05449
	$\alpha = \frac{\pi}{2}$		$\alpha = \frac{2\pi}{3}$		$\alpha = \frac{3\pi}{4}$		$\alpha = \frac{5\pi}{6}$	
θ	$\underline{C}_\Gamma^{M,\text{Tr}}$	$\tilde{C}_\Gamma^{\text{Tr}}$	$\underline{C}_\Gamma^{M,\text{Tr}}$	$\tilde{C}_\Gamma^{\text{Tr}}$	$\underline{C}_\Gamma^{M,\text{Tr}}$	$\tilde{C}_\Gamma^{\text{Tr}}$	$\underline{C}_\Gamma^{M,\text{Tr}}$	$\tilde{C}_\Gamma^{\text{Tr}}$
$\pi/6$	0.93123	2.05449	1.07244	2.39471	1.21573	2.95902	1.47044	4.21999
$\pi/4$	0.93123	1.38951	1.07244	1.64324	1.21573	2.01841	1.47044	2.80588
$\pi/3$	0.78904	1.06349	0.91773	1.27423	1.04309	1.50833	1.26357	2.11790
$\pi/2$	0.75199	0.75200	0.86459	0.86463	0.98220	1.12971	1.19017	1.67033
$2\pi/3$	0.86463	1.06349	0.96174	1.27423	1.08134	1.50833	1.30191	2.11790
$3\pi/4$	0.98220	1.38951	1.07921	1.64324	1.20686	2.01841	1.44721	2.80588
$5\pi/6$	1.19017	2.05449	1.29582	2.39471	1.44268	2.95902	1.72383	4.21999

Table 6: $\underline{C}_\Gamma^{M,\text{Tr}}$ ($M(N) = 124$) and $\tilde{C}_\Gamma^{\text{Tr}}$ for different $\theta, \alpha \in (0, \pi)$.

the paper [9]. Constants in functional (embedding) inequalities arise in a posteriori error estimates of the functional type (error majorants). The details concerning last application can be found [35, 20, 25, 36, 37, 34, 38] and other references cited therein. Below, we deduce an advanced version of an error majorant, which uses constants in Poincaré-type inequalities for functions with zero mean traces on inter-element boundaries. This is done in order to

maximally extend the space of admissible fluxes. However, first, we shall discuss the reasons that invoke Poincaré-type constants in a posteriori estimates.

Let u denote the exact solution of an elliptic boundary value problem generated by the pair of conjugate operators grad and $-\text{div}$ (e.g., the problem (38)–(41) considered below) and v be a function in the energy space satisfying the prescribed (Dirichlet) boundary conditions. Typically, the error $e := u - v$ is measured in terms of the energy norm $\|\nabla e\|$ (or some other equivalent norm), whose square is bounded from above by the quantities

$$\int_{\Omega} R(v, \text{div} q) e \, dx, \quad \int_{\Omega} D(\nabla v, q) \cdot \nabla e \, dx, \quad \text{and} \quad \int_{\Gamma_N} R_{\Gamma_N}(v, q \cdot n) e \, ds,$$

where Ω Lipschitz bounded domain, Γ_N is the Neumann part of the boundary $\partial\Omega$ with the outward unit normal vector n , and q is an approximation of the dual variable (flux). The terms R , D , and R_{Γ_N} represent residuals of the differential (balance) equation, constitutive (duality) relation, and Neumann boundary condition, respectively. Since v and q are known from a numerical solution, fully computable estimates can be obtained if these integrals are estimated by the Hölder, Friedrichs, and trace inequalities (which involve the corresponding constants). However, for Ω with piecewise smooth (e.g., polynomial) boundaries these constants may be unknown. A way to avoid these difficulties is suggested by modifications of the estimates using ideas of domain decomposition. Assume that Ω is a polygonal (polyhedral) domain decomposed into a collection of non-overlapping convex polygonal sub-domains Ω_i , i.e.,

$$\bar{\Omega} := \bigcup_{\Omega_i \in \mathcal{O}_{\Omega}} \bar{\Omega}_i, \quad \mathcal{O}_{\Omega} := \left\{ \Omega_i \in \Omega \mid \Omega_{i'} \cap \Omega_{i''} = \emptyset, \, i' \neq i'', \, i = 1, \dots, N \right\}.$$

We denote the set of all edges (faces) by \mathcal{G} and the set of all interior faces by \mathcal{G}_{int} (i.e., $\Gamma_{ij} \in \mathcal{G}_{\text{int}}$, if $\Gamma_{ij} = \bar{\Omega}_i \cap \bar{\Omega}_j$). Analogously, \mathcal{G}_N denotes the set of edges on Γ_N . The latter set is decomposed into $\Gamma_{N_k} := \Gamma_N \cap \partial\Omega_k$ (the number of faces that belongs to \mathcal{G}_N is K_N). Now, the integrals associated with R and R_{Γ_N} can be replaced by sums of local quantities

$$\sum_{\Omega_i \in \mathcal{G}_{\Omega_i}} \int_{\Omega_i} R_{\Omega_i}(v, \text{div} q) e \, dx, \quad \text{and} \quad \sum_{\Gamma_{N_k} \in \mathcal{G}_N} \int_{\Gamma_{N_k}} R_{\Gamma_N}(v, q \cdot n) e \, ds.$$

If the residuals satisfy the conditions

$$\int_{\Omega_i} R_{\Omega_i}(v, \text{div} q) \, dx = 0 \quad \forall i = 1, \dots, N,$$

and

$$\int_{\Gamma_{N_k}} R_{\Gamma_N}(v, q \cdot n) \, ds = 0, \quad \forall k = 1, \dots, K_N,$$

then

$$\int_{\Omega_i} R_{\Omega}(v, \text{div} q) e \, dx \leq C_{\Omega_i}^{\text{P}} \|R_{\Omega_i}(v, \text{div} q)\|_{\Omega_i} \|\nabla e\|_{\Omega_i} \quad (35)$$

and

$$\int_{\Gamma_{N_k}} R_{\Gamma_N}(v, q \cdot n) e \, ds \leq C_{\Gamma_{N_k}}^{\text{Tr}} \|R_{\Gamma_N}(v, q \cdot n)\|_{\Gamma_{N_k}} \|\nabla e\|_{\Omega_k}. \quad (36)$$

Hence, we can deduce a computable upper bound of the error that contains local constants $C_{\Omega_i}^{\text{P}}$ and $C_{\Gamma_{N_k}}^{\text{Tr}}$ for simple subdomains (e.g., triangles or tetrahedrons) instead of the global constants associated with Ω .

The constant C_{Ω}^{P} may arise if, e.g., nonconforming approximations are used. For example, if v does not exactly satisfy the Dirichlet boundary condition on Γ_{D_k} , then in the process of estimation it may be necessary to evaluate terms of the type

$$\int_{\Gamma_{D_k}} G_D(v) e \, ds, \quad k = 1, \dots, K_D,$$

where Γ_{D_k} is a part of Γ_D associated with a certain Ω_k , and $G_D(v)$ is a residual generated by inexact satisfaction of the boundary condition. If we impose the requirement that the Dirichlet boundary condition is satisfied in a weak sense, i.e., $\{G_D(v)\}_{\Gamma_{D_k}} = 0$, then each boundary integral can be estimated as follows:

$$\int_{\Gamma_{D_k}} G_D(v) e \, ds \leq C_{\Gamma_{D_k}}^{\text{P}} \|G_D(v)\|_{\Gamma_{D_k}} \|\nabla e\|_{\Omega_k}. \quad (37)$$

After summing up (35), (36), and (37), we obtain a product of weighted norms of localized residuals (which are known) and $\|\nabla e\|_\Omega$. Since the sum is bounded from below by the squared energy norm, we arrive at computable error majorant.

Now, we discuss elaborately these questions within the paradigm of the following boundary value problem: find u such that

$$-\operatorname{div} p + \varrho^2 u = f, \quad \text{in } \Omega, \quad (38)$$

$$p = A \nabla u, \quad \text{in } \Omega, \quad (39)$$

$$u = u_D, \quad \text{on } \Gamma_D, \quad (40)$$

$$A \nabla u \cdot n = F \quad \text{on } \Gamma_N. \quad (41)$$

Here $f \in L^2(\Omega)$, $F \in L^2(\Gamma_N)$, $u_D \in H^1(\Omega)$, and A is a symmetric positive definite matrix with bounded coefficients satisfying the condition $\lambda_1 |\xi|^2 \leq A \xi \cdot \xi$, where λ_1 is a positive constant independent of ξ . The generalized solution of (38)–(41) exists and is unique in the set $V_0 + u_D$, where $V_0 := \{w \in H^1(\Omega) \mid w = 0 \text{ on } \Gamma_D\}$.

Assume that $v \in V_0 + u_D$ is a conforming approximation of u . We wish to find a computable majorant of the error norm

$$\|e\|^2 := \|\nabla e\|_A^2 + \|\varrho e\|^2, \quad (42)$$

where $\|\nabla e\|_A^2 := \int_\Omega A \nabla e \cdot \nabla e \, dx$. First, we note that the integral identity that defines u can be rewritten in the form

$$\int_\Omega A \nabla e \cdot \nabla w \, dx + \int_\Omega \varrho^2 e w \, dx = \int_\Omega (f w - \varrho^2 v w - A \nabla v \cdot \nabla w) \, dx + \int_{\Gamma_N} F w \, ds, \quad \forall w \in V_0. \quad (43)$$

It is well known (see Section 4.2 in [35]) that this relation yields a computable majorant of $\|e\|^2$, if we introduce a vector-valued function $q \in H(\Omega, \operatorname{div})$, such that $q \cdot n \in L^2(\Omega)$, and transform (43) by means of integration by parts relations. The majorant has the form

$$\|e\| \leq \|D_\Omega(\nabla v, q)\|_{A^{-1}} + C_1 \|R(v, \operatorname{div} q)\|_\Omega + C_2 \|R_{\Gamma_N}(v, q \cdot n)\|_{\Gamma_N}, \quad (44)$$

where C_1 and C_2 are positive constants explicitly defined by λ_1 , the Friedrichs' constant C_Ω^F in inequality $\|v\|_\Omega \leq C_\Omega^F \|\nabla v\|_\Omega$ for functions vanishing on Γ_D , and constant $C_{\Gamma_N}^{\operatorname{Tr}}$ in the trace inequality associated with Γ_N . The integrands are defined by the relations

$$D(\nabla v, q) := A \nabla v - q, \quad R(v, \operatorname{div} q) := \operatorname{div} q + f - \varrho^2 v, \quad \text{and} \quad R_{\Gamma_N}(v, q \cdot n) := q \cdot n - F.$$

In general, finding C_Ω^F and $C_{\Gamma_N}^{\operatorname{Tr}}$ may not be an easy task. We can exclude C_2 if q additionally satisfies the condition $q \cdot n = F$. Then, the last term in (44) vanishes. However, this condition is difficult to satisfy, if F is a complicated nonlinear function. In order to exclude C_1 together with C_2 , we can apply domain decomposition technique and use (35) instead of the global estimate. Then, the estimate will operate with the constants $C_{\Omega_i}^F$ (whose upper bounds are known for convex domains). Moreover, it is shown below that by using the inequalities (2) and (4), we can essentially weaken the assumptions required for the variable q .

Define the space of vector-valued functions

$$\begin{aligned} \hat{H}(\Omega, \mathcal{O}_\Omega, \operatorname{div}) := & \left\{ q \in L^2(\Omega, \mathbb{R}^d) \mid q = q_i \in H(\Omega_i, \operatorname{div}), \{ \operatorname{div} q_i + f - \varrho^2 v \}_{\Omega_i} = 0, \quad \forall \Omega_i \in \mathcal{O}_\Omega, \right. \\ & \{ (q_i - q_j) \cdot n_{ij} \}_{\Gamma_{ij}} = 0, \quad \forall \Gamma_{ij} \in \mathcal{G}_{\operatorname{int}}, \\ & \left. \{ q_i \cdot n_k - F \}_{\Gamma_{N_k}} = 0, \quad \forall k = 1, \dots, K_N \right\}. \end{aligned}$$

We note that the space $\hat{H}(\Omega, \mathcal{O}_\Omega, \operatorname{div})$ is wider than $H(\Omega, \operatorname{div})$ (so that we have more flexibility in determination of optimal reconstruction of numerical fluxes). Indeed, the vector-valued functions in $H(\Omega, \operatorname{div})$ must have continuous normal components on all $\Gamma_{ij} \in \mathcal{G}_{\operatorname{int}}$ and satisfy the Neumann boundary condition in the pointwise sense. The functions in $\hat{H}(\Omega, \mathcal{O}_\Omega, \operatorname{div})$ satisfy much weaker conditions: namely, the normal components are continuous only in terms of mean values (integrals) and the Neumann condition must hold in the integral sense only.

We reform (43) by means of the integral identity

$$\sum_{\Omega_i \in \mathcal{O}_\Omega} \int_{\Omega_i} (q \cdot \nabla w + \operatorname{div} q w) \, dx = \sum_{\Gamma_{ij} \in \mathcal{G}_{\operatorname{int}}} \int_{\Gamma_{ij}} (q_i - q_j) \cdot n_{ij} w \, ds + \sum_{\Gamma_{N_k} \in \Gamma_N} \int_{\Gamma_{N_k}} q_i \cdot n_i w \, ds,$$

which holds for any $w \in V_0$ and $q \in \hat{H}(\Omega, \mathcal{O}_\Omega, \text{div})$. By setting $w = e$ in (43) and applying the Hölder inequality, we find that

$$\begin{aligned} \|e\|^2 \leq & \|D(\nabla v, q)\|_{A^{-1}} \|\nabla e\|_A + \sum_{\Omega_i \in \mathcal{O}_\Omega} \|R(v, \text{div} q)\|_{\Omega_i} \|e - \{e\}_{\Omega_i}\|_{\Omega_i} \\ & + \sum_{\Gamma_{ij} \in \mathcal{G}_{\text{int}}} r_{ij}(q) \|e - \{e\}_{\Gamma_{ij}}\|_{\Gamma_{ij}} + \sum_{\Gamma_{N_k} \in \Gamma_N} \rho_k(q) \|e - \{e\}_{\Gamma_{N_k}}\|_{\Gamma_{N_k}}, \end{aligned}$$

where

$$r_{ij}(q) := \|(q_i - q_j) \cdot n_{ij}\|_{\Gamma_{ij}} \quad \text{and} \quad \rho_k(q) := \|q_k \cdot n_k - F\|_{\Gamma_{N_k}}.$$

In view of (1) and (4), we obtain

$$\begin{aligned} \|e\|^2 \leq & \|D(\nabla v, q)\|_{A^{-1}} \|\nabla e\|_A + \sum_{\Omega_i \in \mathcal{O}_\Omega} \|R(v, \text{div} q)\|_{\Omega_i} C_{\Omega_i}^{\text{P}} \|\nabla e\|_{\Omega_i} \\ & + \sum_{\Gamma_{ij} \in \mathcal{G}_{\text{int}}} r_{ij}(q) C_{\Gamma_{ij}}^{\text{Tr}} \|\nabla e\|_{\Omega_i} + \sum_{\Gamma_{N_k} \in \Gamma_N} \rho_k(q) C_{\Gamma_{N_k}}^{\text{Tr}} \|\nabla e\|_{\Omega_i}. \quad (45) \end{aligned}$$

The second term in the right hand side is estimated by the quantity $\mathfrak{R}_1(v, q) \|\nabla e\|_\Omega$, where

$$\mathfrak{R}_1^2(v, q) := \sum_{\Omega_i \in \mathcal{O}_\Omega} \frac{(\text{diam } \Omega_i)^2}{\pi^2} \|R(v, \text{div} q)\|_{\Omega_i}^2.$$

We can represent any $\Omega_i \in \mathcal{O}_\Omega$ as a sum of simplexes such that each simplex has one edge on $\partial\Omega_i$. Let $C_{i, \text{max}}^{\text{Tr}}$ denote the largest constant in the respective Poincaré-type inequalities (4) associated with all edges of $\partial\Omega_i$. Then, the last two terms of (45) can be estimated by the quantity $\mathfrak{R}_2(v, q) \|\nabla e\|_\Omega$, where

$$\mathfrak{R}_2^2(q) := \sum_{\Omega_i \in \mathcal{O}_\Omega} (C_{i, \text{max}}^{\text{Tr}})^2 \eta_i^2, \quad \text{with} \quad \eta_i^2 = \sum_{\substack{\Gamma_{ij} \in \mathcal{G}_{\text{int}} \\ \Gamma_{ij} \cap \partial\Omega_i \neq \emptyset}} \frac{1}{4} r_{ij}^2(q) + \sum_{\substack{\Gamma_k \in \mathcal{G}_N \\ \Gamma_k \cap \partial\Omega_i \neq \emptyset}} \rho_k^2(q).$$

Then, (45) yields the estimate

$$\|e\|^2 \leq \|D(\nabla v, q)\|_{A^{-1}} \|\nabla e\|_A + (\mathfrak{R}_1(v, q) + \mathfrak{R}_2(q)) \|\nabla e\|_\Omega,$$

which shows that

$$\|e\| \leq \|D(\nabla v, q)\|_{A^{-1}} + \frac{1}{\lambda_1} \left(\mathfrak{R}_1(v, q) + \mathfrak{R}_2(q) \right). \quad (46)$$

Here, the term $\mathfrak{R}_2(q)$ controls violations of conformity of q (on interior edges) and inexact satisfaction of boundary conditions (on edges related to Γ_N). It is easy to see that $\mathfrak{R}_2(q) = 0$, if and only if the quantity $q \cdot n$ is continuous on \mathcal{G}_{int} and exactly satisfies the boundary condition. Hence, $\mathfrak{R}_2(q)$ can be viewed as a measure of the ‘flux nonconformity’. Other terms have the same meaning as in well-known a posteriori estimates of the functional type, namely, the first term measures the violations of the relation $q = A\nabla v$ (cf. (39)), and $\mathfrak{R}_1(v, q)$ measures inaccuracy in the equilibrium (balance) equation (38). The right-hand side of (46) contains known functions (approximations v and q of the exact solution and exact flux). The constants $C_{i, \text{max}}^{\text{Tr}}$ can be easily computed using results of Section 2-4. Finally, we note that estimates similar to (46) were derived in [36] for elliptic variational inequalities and in [25] for a class of parabolic problems.

References

- [1] M. Ainsworth and J. T. Oden. *A posteriori error estimation in finite element analysis*. Wiley and Sons, New York, 2000.
- [2] I. Babuška and A. K. Aziz. On the angle condition in the finite element method. *SIAM J. Numer. Anal.*, 13(2):214–226, 1976.
- [3] C. Bandle. *Isoperimetric inequalities and applications*, volume 7 of *Monographs and Studies in Mathematics*. Pitman (Advanced Publishing Program), Boston, Mass.-London, 1980.
- [4] R. Bañuelos, T. Kulczycki, I. Polterovich, and B. Siudeja. Eigenvalue inequalities for mixed Steklov problems. In *Operator theory and its applications*, volume 231 of *Amer. Math. Soc. Transl. Ser. 2*, pages 19–34. Amer. Math. Soc., Providence, RI, 2010.

- [5] P. H. Bérard. Spectres et groupes cristallographiques. I. Domaines euclidiens. *Invent. Math.*, 58(2):179–199, 1980.
- [6] D. Braess. *Finite elements*. Cambridge University Press, Cambridge, second edition, 2001. Theory, fast solvers, and applications in solid mechanics, Translated from the 1992 German edition by Larry L. Schumaker.
- [7] C. Carstensen and S. A. Funken. Fully reliable localized error control in the FEM. *SIAM J. Sci. Comput.*, 21(4):1465–1484, 2000.
- [8] C. Carstensen and J. Gedicke. Guaranteed lower bounds for eigenvalues. *Math. Comp.*, 83(290):2605–2629, 2014.
- [9] C. Carstensen and S. A. Sauter. A posteriori error analysis for elliptic PDEs on domains with complicated structures. *Numer. Math.*, 96(4):691–721, 2004.
- [10] S. Y. Cheng. Eigenvalue comparison theorems and its geometric applications. *Math. Z.*, 143(3):289–297, 1975.
- [11] P. G. Ciarlet. *The finite element method for elliptic problems*. North-Holland Publishing Co., Amsterdam-New York-Oxford, 1978. Studies in Mathematics and its Applications, Vol. 4.
- [12] C. R. Dohrmann, A. Klawonn, and O. B. Widlund. Domain decomposition for less regular subdomains: overlapping Schwarz in two dimensions. *SIAM J. Numer. Anal.*, 46(4):2153–2168, 2008.
- [13] D. W. Fox and J. R. Kuttler. Sloshing frequencies. *Z. Angew. Math. Phys.*, 34(5):668–696, 1983.
- [14] A. Girouard and I. Polterovich. Spectral geometry of the steklov problem. *arXiv.org*, math/1411.6567, 2014.
- [15] Y. Hoshikawa and H. Urakawa. Affine Weyl groups and the boundary value eigenvalue problems of the Laplacian. *Interdiscip. Inform. Sci.*, 16(1):93–109, 2010.
- [16] A. Klawonn, O. Rheinbach, and O. B. Widlund. An analysis of a FETI-DP algorithm on irregular subdomains in the plane. *SIAM J. Numer. Anal.*, 46(5):2484–2504, 2008.
- [17] V. Kozlov and N. Kuznetsov. The ice-fishing problem: the fundamental sloshing frequency versus geometry of holes. *Math. Methods Appl. Sci.*, 27(3):289–312, 2004.
- [18] V. Kozlov, N. Kuznetsov, and O. Motygin. On the two-dimensional sloshing problem. *Proc. R. Soc. Lond. Ser. A Math. Phys. Eng. Sci.*, 460(2049):2587–2603, 2004.
- [19] N. Kuznetsov, T. Kulczycki, M. Kwaśnicki, A. Nazarov, S. Poborchi, I. Polterovich, and B. Siudeja. The legacy of Vladimir Andreevich Steklov. *Notices Amer. Math. Soc.*, 61(1):9–22, 2014.
- [20] U. Langer, S. Repin, and M. Wolfmayr. Functional a posteriori error estimates for parabolic time-periodic boundary value problems. *CMAM*, 15(3):353–372, 2015.
- [21] R. S. Laugesen and B. A. Siudeja. Maximizing Neumann fundamental tones of triangles. *J. Math. Phys.*, 50(11):112903, 18, 2009.
- [22] R. S. Laugesen and B. A. Siudeja. Minimizing Neumann fundamental tones of triangles: an optimal Poincaré inequality. *J. Differential Equations*, 249(1):118–135, 2010.
- [23] X. Liu and S. Oishi. Guaranteed high-precision estimation for P_0 interpolation constants on triangular finite elements. *Jpn. J. Ind. Appl. Math.*, 30(3):635–652, 2013.
- [24] A. Logg, K.-A. Mardal, and G. N. Wells, editors. *Automated solution of differential equations by the finite element method*, volume 84 of *Lecture Notes in Computational Science and Engineering*. Springer, Heidelberg, 2012. The FEniCS book.
- [25] S. Matculevich, P. Neittaanmäki, and S. Repin. A posteriori error estimates for time-dependent reaction-diffusion problems based on the Payne–Weinberger inequality. *AIMS*, 35(6), 2015.
- [26] B. J. McCartin. Eigenstructure of the equilateral triangle. II. The Neumann problem. *Math. Probl. Eng.*, 8(6):517–539, 2002.
- [27] S. G. Mikhlin. *Constants in some inequalities of analysis*. A Wiley-Interscience Publication. John Wiley and Sons, Ltd., Chichester, 1986. Translated from the Russian by Reinhard Lehmann.

- [28] M. T. Nakao and N. Yamamoto. A guaranteed bound of the optimal constant in the error estimates for linear triangular element. In *Topics in numerical analysis*, volume 15 of *Comput. Suppl.*, pages 165–173. Springer, Vienna, 2001.
- [29] A. I. Nazarov and S. I. Repin. Exact constants in Poincaré type inequalities for functions with zero mean boundary traces. *Mathematical Methods in the Applied Sciences*, 2014. Published in arXiv.org in 2012, math/1211.2224.
- [30] L. E. Payne and H. F. Weinberger. An optimal Poincaré inequality for convex domains. *Arch. Rational Mech. Anal.*, 5:286–292 (1960), 1960.
- [31] M. A. Pinsky. The eigenvalues of an equilateral triangle. *SIAM J. Math. Anal.*, 11(5):819–827, 1980.
- [32] H. Poincaré. Sur les Equations aux Derivees Partielles de la Physique Mathematique. *Amer. J. Math.*, 12(3):211–294, 1890.
- [33] H. Poincaré. Sur les Equations de la Physique Mathematique. *Rend. Circ. Mat. Palermo*, 8:57–156, 1894.
- [34] S. Repin. A posteriori error estimation for variational problems with uniformly convex functionals. *Math. Comput.*, 69(230):481–500, 2000.
- [35] S. Repin. *A posteriori estimates for partial differential equations*, volume 4 of *Radon Series on Computational and Applied Mathematics*. Walter de Gruyter GmbH & Co. KG, Berlin, 2008.
- [36] S. Repin. Estimates of deviations from exact solutions of variational inequalities based upon payne-weinberger inequality. *J. Math. Sci. (N. Y.)*, 157(6):874–884, 2009.
- [37] S. Repin. Estimates of constants in boundary-mean trace inequalities and applications to error analysis. In *Numerical Mathematics and Advanced Applications - ENUMATH 2013*, volume 103 of *Lecture Notes in Computational Science and Engineering*, pages 215–223. Springer, Switzerland, 2015.
- [38] S. I. Repin and L. S. Xanthis. A posteriori error estimation for elastoplastic problems based on duality theory. *Comput. Methods Appl. Mech. Engrg.*, 138(1-4):317–339, 1996.
- [39] V. A. Steklov. Sur les problèmes fondamentaux de la physique mathematique. *Ann. Sci. Ec. Norm. Supér.*, 3(19):191–259, 455–490, 1902.
- [40] Inc. ©1994-2015 The MathWorks. Mathworks. products and services, 2015.
- [41] A. Toselli and O. Widlund. *Domain decomposition methods—algorithms and theory*, volume 34 of *Springer Series in Computational Mathematics*. Springer-Verlag, Berlin, 2005.
- [42] R. Verfürth. *A review of a posteriori error estimation and adaptive mesh-refinement techniques*. Wiley and Sons, Teubner, New-York, 1996.

